ABSTRACT

Title of Thesis:	EVALUATING WHITE PERCH (MORONE AMERICANA) FECUNDITY IN SELECT CHESAPEAKE BAY TRIBUTARIES IN RESPONSE TO PATHOLOGY AND FITNESS
	Jacob Thomas Shaner, Master of Science, 2020
Thesis Directed By:	Professor Reginal M. Harrell, Marine Estuarine and Environmental Sciences Program

Fecundity studies have emerged as a complement to generalized stock assessment methods in an effort to more accurately determine reproductive potential, as well as explain a lack of stock recovery in some cases. The Chesapeake Bay presents an interesting case study, in that widespread anthropogenic influence has created the potential to reduce reproductive fitness among resident species, including white perch (*Morone americana*). This study seeks to investigate white perch population fecundity in response to habitat quality, as well as disease and nutrition, through the use of stereological and automated counting methods to assess agreement between stock assessments and reproductive potential. Results indicate lack of impact on fecundity from degraded habitat, limited impact of individual nutrition, and no conclusive effect from disease. These findings, coupled with stable recruitment, indicate that white perch reproduction in the Chesapeake Bay is unaffected by increased population stress.

EVALUATING WHITE PERCH (MORONE AMERICANA) FECUNDITY IN SELECT CHESAPEAKE BAY TRIBUTARIES IN RESPONSE TO PATHOLOGY AND FITNESS

by

Jacob Thomas Shaner

Thesis submitted to the Faculty of the Graduate School of the
University of Maryland, College Park, in partial fulfillment
of the requirements for the degree of
Master of Science
2020

Advisory Committee:
Professor Reginal Harrell, Chair
Dr. John Jacobs
Dr. Lance Yonkos

Dedication

For Marjorie Alice Wisse (Stowe)

“Fish eggs? Gaak”

And

John Robert Stowe

Acknowledgements

This research would not have been possible without the generous support of numerous individuals and organizations. First and foremost, I would like to thank the members of my research committee, who took time out of their incredibly busy schedules to help me through the process of planning and executing this project. I owe this degree to the willingness of Reggie Harrell to take me on as a student and to provide resources for the completion my studies. He was always willing to answer questions any time they might pop into my head, and helped me navigate the interesting circumstances of doing a project with State of Maryland data over which I had very little control. John Jacobs was an essential part of my committee, and also my in-lab "go-to" for all things quantitative. He has a knack for playing a mean lead guitar as well, with band rehearsal always helping to reduce stress. Lance Yonkos provided integral help in the planning of the final project, and I owe him much thanks for agreeing to step in at the last minute to fill a void in the committee.

I would also like to thank employees of Maryland DNR (MDNR), including Barbara Johnston and Brian Richardson with the Aquatic Animal Health Program for agreeing to let me do this, Chuck Stence, Matt Baldwin, and Ashlee Horne with Anadromous Restoration for always lending a hand and a shock boat (or spare outboard), Amanda Weschler and Cindy Driscoll with the Stranding Program for working around my schedule, Carol McCollough, Stu Lehmann and everyone with the MDNR Histology department, and of course Kevin Rosemary and Mark Matsche with Wild Fish Health for incalculable support in the lab and field. Field help was also provided by Mike Mangold and Steve Minkkinen of the United States Fish and Wildlife Service (USFWS) Chesapeake Bay Office, as well as Charles Poukish and

Chris Luckett of the Maryland Department of the Environment (MDE) Fish Health team. Out-of-state collections were thanks to the hard work of Troy Tuckey and Wendy Lowery of The Virginia Institute of Marine Science (VIMS), Lance Butler and Joe Perillo of the Philadelphia Water Department, and Jim Bulak and his team from South Carolina Department of Natural Resources (SCDNR).

I will also need to thank family members and friends for helping to keep a smile on my face through part-time degree work and full-time work, especially Tom, Carolyn and Morgann Shaner, and Suzanne Sullivan. There is no chance I would have finished this without all of your support and help. Cannot wait to share the next chapter with you all.

This study was carried out using the Maryland Department of Natural Resources protocols for animal care and use as the animals were part of a greater MDNR stock assessment study.

Table of Contents

List of Tables

Chapter 2

Chapter 3

(TW+A). Mycobacteriosis as a covariate exerts a strong influence on model performance with the base model showing >14 ΔAICc when compared.

Table 3.6 Addition to base model (Total weight+age) of Severn River samples as a covariate ("River"), to determine if populations in a comparatively degraded habitat are affected by increases in total disease pathology and stress. Selection procedures show weak evidence of difference (<1 ΔAICc).

Table 3.7 Variance inflation factor (VIF) results for each model used in analysis, by variable. Variables include total weight (TW), age (A), condition factor (K), observed body fat index (BFI), total health assessment index score (HAI), hepatosomatic index (HSI), mycobacteriosis presence (AF) and location (L). VIF factors are below conservative thresholds of 2.5, indicating no collinearity.

Table 3.8 Omega squared (ω^2) effect size results for each model used in analysis, by variable. Variables include total weight (TW), age (A), condition factor (K), observed body fat index (BFI), total health assessment index score (HAI), hepatosomatic index (HSI), mycobacteriosis presence (AF) and location (L). Effect ranked as per Field (2013) with 0.01 = small, 0.06 = medium, ≥0.14 = large.

Appendix I

Table A.1 Example of pilot study fecundity data, obtained stereologically, with observed coefficient of error (OCE) calculations. Separate OCE percentages were needed for both area calculations and number counts. The goal of pilot studies was to keep error rates below 10% by adjusting number of grid fields counted per specimen.

List of Figures

Chapter 2

Chapter 1: Introduction

1.1 Life History and Distribution

White perch *Morone americana* are endemic to the Chesapeake Bay region, inhabiting both brackish and fresh waters of the Maryland Chesapeake Bay. The distribution of white perch is widespread in the Mid-Atlantic region of the United States, with a spatial range from Newfoundland to the sub-tropical waters of the US Atlantic coast (Setzler-Hamilton 1991). Other population segments exist in the Great Lakes but are non-native and are the result of introductions due to commerce and other human activities (Scott et al. 1963, Busch et al. 1977).

A semi-anadromous species, white perch migrate as part of spawning behavior but maintain relatively small home ranges, making them an ideal candidate for study of environmental comparison (Mansueti 1961, McGrath and Austin 2009). Migrations begin in early spring months for the purposes of spawning, coupled with return migrations to primary foraging locations in summer, and finally moving to deeper waters for over-wintering (Mansueti 1961, Richkus and Stroup 1987, McGrath and Austin 2009). White perch are a known structure dwelling species that frequent both natural and artificial structures in search of prey (Richkus and Stroup 1987). Ideal hydrological conditions may vary for white perch populations based on home range, as they have been shown to be generalist in terms of habitat selection and life history requirements (Setzler-Hamilton 1991). They typically inhabit water of salinities between 5-18 ppt, although evidence suggests there are freshwater (0-0.8 ppt) contingents of the larger Chesapeake Bay subpopulation in tidal rivers (Stanley and Danie 1983, Kraus and Secor 2004). Sampling by the Maryland Department of

Environment (MDE) and the Maryland Department of Natural Resources (MDNR) has further discovered isolated freshwater populations in a number of Maryland's freshwater reservoirs (Poukish 2017).

In terms of population abundance, MDNR maintains recruitment indices to monitor the population status of white perch in the Bay due to their ecological and commercial importance. Ecologically, white perch are of importance given their relative abundance and trophic position as a secondary consumer (Setzler-Hamilton 1991). Larval white perch are planktivorous, and serve as important prey for a number of freshwater species, notably Bluegill *Lepomis macrochirus* (Margulies 1990). As white perch progress through maturation, individuals become more piscivorous but also continue to serve as prey for larger teleost species. Striped bass *Morone saxitilis* and possibly other piscivores such as bluefish *Pomatomus saltatrix* prey on white perch in the Chesapeake, with white perch in some cases constituting up to 25% of the diet of striped bass in tidal freshwater habitats (Walter and Austin 2003). As of yet, it is not known whether white perch are important prey for introduced species such as blue catfish *Ictalurus furcatus* and snakehead *Channa spp*. In the Maryland Chesapeake Bay, white perch also support important recreational and commercial fisheries, with combined landings of approximately 2.4 million pounds in 2016 (Piavis and Webb 2017).

1.2 Reproduction and Recruitment

In the Chesapeake Bay, white perch typically reach sexual maturity at year 3, although some differences between the sexes may exist (Mansueti 1961). Spawning involves micro-migrations in discrete riverine systems, generally to shallower, less saline upstream regions (Mansueti 1961, Kraus and Secor 2004, McGrath 2009).

Spawning behaviors are specifically stimulated by water temperature changes (Stanley and Danie 1983), with optimal spawning temperatures in the Bay of approximately 12-14 C° (Setzler-Hamilton 1991). White perch are iteroparous and utilize a broadcast spawning strategy, relying on congregation of individuals to facilitate pelagic fertilization. Compared to fish of similar size, white perch typically have higher oocyte counts per gonad volume (Setzler-Hamilton 1991). Fecundity however, varies widely on an individual basis and has been shown to also vary geographically, with estimates ranging from 20,304-90,147 eggs per fish in North Carolina, 50,000-150,000 in the Chesapeake Bay, and higher counts of up to 280,000 in Delaware Bay (Setzler-Hamilton 1991, Okoye et al. 2008). Combining all available data creates a range of 5,000 to 320,000 eggs with a mean of 40,000 eggs per female (Klauda et al. 1988, Setzler-Hamilton 1991, Okoye et al. 2008). Age also is an important co-variant with fecundity, as older fish have higher observed fecundity (Mansueti 1961, 1964, Okoye et al. 2008). Ovarian maturation follows a seasonal pattern, with largest gonad size, as measured by gonadosomatic index (GSI) of gonad mass to body mass, found during spawning season, which in the Mid-Atlantic is typically April (Jackson and Sullivan 1995). Oocyte size distributions of white perch are predictive of spawning state. When spawning nears, oocyte sizes exhibit a multimodal distribution, indicating that white perch are group-synchronous or asynchronous spawners, with multiple clutches of eggs mixed throughout the ovaries in two or more distinct size groups (Jackson and Sullivan 1995, Blazer 2002, Murua et al. 2003). It is hypothesized that white perch are determinate spawners, where mature fish fully-spawn viable oocytes every season (Jackson and Sullivan 1995). It is believed that unspawned pre-vitellogenic oocytes are resorbed in white

perch (Jackson and Sullivan 1995). Vitellogenic white perch eggs are generally 0.79-0.90 mm in diameter unfertilized, with a single oil globule and flattened attachment disc (Mansueti 1964).

1.3 Environmental Effects on Reproduction and Overall Health

One of the principal reasons for revisiting the fecundity of *M. americana* in the Chesapeake Bay in this current study is the widespread environmental change that has occurred since the last studies were conducted. Increased development in the watershed has changed hydrological regimes and increased runoff, leading to degradations in both benthic and pelagic habitat quality (Dauer et al. 2000, Uphoff et al. 2011). In addition, changes in agricultural practices, such as increased development of concentrated livestock operations and use of chemical fertilizer, have changed nitrogen and phosphorous inputs into the watershed, often creating hypoxic and anoxic conditions, which have been linked to rising stress and disease rates in fish (Boynton et al. 1995, Boesch et al. 2000, Barton et al. 2002, USEPA 2010, Lapointe et al. 2014). Stress levels among fish individuals and populations is important, as chronic stress can contribute to reproductive effects such as reduced fecundity or progeny survival (Greeley 2002). While many of these effects are Bay-wide in the Chesapeake, the more discrete impacts of local land-use, including contaminant loading and sediment run-off are of special concern to white perch populations given their discrete home ranges (McLaughlin et al. 2018). The primary riverine comparison of this study between the Severn and Choptank Rivers highlights the different impacts that land-use could potentially have on living resources. Numerous studies have linked land-use patterns in the Chesapeake region to the health of local biota, including PCB loading in white perch, tumor incidence in brown

bullhead *Ameiurus nebulosus*, changes in yellow perch *Perca flavescens* gonad morphologies and health, and presence of intersex in Pennsylvania largemouth bass *Micropterus salmoides* (King et al. 2004, Pinkney et al. 2011, Blazer et al. 2013, 2014).

In general, increases in contaminant loading from both point and diffuse sources of pollution have been shown to decrease condition indices in teleost species in the Chesapeake Bay watershed (Morgan et al. 1973, Adams et al. 1996, McLaughlin et al. 2018). Using an adapted habitat health assessment index first used in the Tennessee Valley to determine point-source pollutant impacts, MDNR has sampled white perch as an indicator species to justify findings of ecosystem health based on land use in Chesapeake Bay sub-estuaries for the past 5 years (Adams et al. 1993, MDNR unpublished data). Data from studies in the Tred Avon River have demonstrated the potential for segments of white perch populations to be impacted in different ways depending on localized anthropogenic impacts (McLaughlin et al. 2018). Fish from headwater sites of the Tred Avon, that have heavier anthropogenic influence from the town of Easton, MD, showed significantly more lesions, specifically splenic machrophage aggregates and intestinal parasites, as well as significantly lower overall white blood cell counts (McLaughlin et al. 2018).

An omission of all MDNR Health Assessment Index work to date however, has been reproductive health. Research in the Chesapeake Bay watershed has determined a number of reproductive effects from exposure to "chemicals of emerging concern", which typically include estrogenic/antiandrogenic compounds (Blazer et al. 2007, Blazer et al. 2013, Yonkos et al. 2014). Examples include intersex in smallmouth bass (*Micropterus dolomieu*) as a result of higher human

population density and higher agricultural intensity, and yellow perch in the Severn River presenting with abnormal yolk appearance, zona pellucida and incomplete maturation of oocytes in response to exposure (Blazer et al. 2007, Blazer et al. 2013). While intersex in white perch has not been exhaustively studied in the Chesapeake Region, white perch have been observed presenting intersex in other regions, which manifests primarily in appearance of ova in testis tissue and high levels of vitellogenin among male specimens (Kavanagh et al. 2004). Given findings of intersex in the same habitat occupied by white perch, albeit in other species, still raises concern for the reproductive health of white perch in the Bay.

PCB contamination is another driver of possible reproductive effects, with certain compounds shown in lab tests to inhibit ovarian development, hormone secretion and larval survival in Atlantic croaker *Micropogonias undulatus*, fathead minnows *Pimephales promelas*, and rainbow trout *Oncorhynchus mykiss* (Monosson et al. 1994). When its effect was studied on white perch using direct injection, specimens experienced suppressed ovarian growth and oocyte development, leading to lower larval survival rates (Monosson et al. 1994). Despite these demonstrated correlations, however, population-level impacts of PCB contamination might be dampened by resilience of the population in question (Barnthouse et al. 2009). While intersex and reproductive stress are extensively studied, research on environmental condition and fecundity is sparse, despite the importance of reproductive potential to recruitment and population health. Possible justification for this paucity of information might center on the observance of confounding effects of contamination, including increased overall fecundity but decreased overall egg size, or increased

rates of oocyte atresia (Greeley 2002). Caution must therefore be exercised when solely using fecundity as an indicator of environmental quality.

Another concern both in ecosystem quality and overall population stress is the potential for parasitic infestation. Parasite abundance in fish has been positively correlated to underlying stress levels, making discovery of a novel coccidian in Maryland white perch populations a possible harbinger of rising stress levels (Overstreet 1997). Maryland DNR staff biologists first noted the novel coccidian parasite *Goussia bayae* in 2016 (Matsche et al. 2019a). Parasites were discovered in hepatic tissue, the gallbladder, and the adjoining common bile duct. Further investigation pinpointed the greatest internal abundance of parasites to be found in bile fluids. Throughout 2017, Maryland DNR personnel collected information regarding abundance, life cycle, and seasonality of *Goussia bayae*. The life cycle follows that of coccidians of the genus *Goussia* with 3 distinct stages, merogony, gamogony and sporogony (Lom and Dyková 1981, Matsche 2019a). Gamogony and sporogony were described through fresh bile observations. When sporulation occurred, each oocyst contained 4 sporocysts with 2 sporozoites per sporocyst (Matsche et al. 2019a). Sporocyst walls are comparatively thick in this species, with morphologies of oocysts further indicating its logical inclusion in the genus *Goussia* (Lom and Dyková 1981, Davies and Ball 1993, Matsche et al. 2019a). The seasonality of the parasite follows a distinct pattern of one peak abundance that coincides with spawning in *M. americana* (Matsche et al. 2019b).

While coccidiosis is common in many other fauna, study of coccidiosis in fish, specifically wild fish, is sparse. Typically, coccidian infections manifest themselves in the gastrointestinal systems of host species, with most infections

appearing to be non-lethal (Lom and Dyková 1981, Davies and Ball 1993). Correlations have been found between liver lesions and rare, extra-intestinal coccidian infections, specifically in *Clupea harengus* in the North Atlantic, with certain infections causing notable destruction of hepatic tissue (Morrison and Hawkins 1984, Davies and Ball 1993, Iwanowicz 2011). It is not reported whether this hepatic infection caused any notable changes in vitellogenin production. White perch in particular have no documented coccidian parasitism until this recent discovery, so effects remain to be seen. This particular genus of coccidia is less studied than most, but documented effects of newly described *Goussia bayae* on the white perch liver, including inflammation and isolated necrosis, may have effects on vitellogenin production and egg viability (Matsche et al. 2019b).

The conservation of reproductive potential is one of the fundamental goals of sustainable fisheries management. Given the broad spectrum of potential anthropogenic and parasitic factors potentially affecting white perch fecundity in the Chesapeake Bay, and given the long gap in study of the species' fecundity in the region, re-evaluation is necessary to determine if white perch are experiencing negative reproductive impacts. This study seeks to test and utilize new tools in fish fecundity sampling to evaluate white perch fecundity, not only to determine the reproductive potential of current riverine sub-populations of Chesapeake Bay white perch, but to also effectively model fecundity as a factor of sampling location and fish health.

Chapter 2: Assessing the validity of using automated and stereological fecundity methods to determine fecundity in white perch (*Morone americana*)

2.1 Abstract

In fisheries management, reproductive output, typically measured with spawning stock biomass, is used to monitor effects of natural and anthropogenic removals and to determine sustainable harvest levels. Fecundity data in particular, can add specificity to measures of spawner abundance to validate recruitment findings, and decipher early warning signs of potential reproductive failure. Whole oocyte counting is the typical benchmark for fecundity estimation, but can prove tedious when performed by ocular methodology and not with particle-counting equipment. The purpose of this study was to test the efficacy of using semi-automation for oocyte counting and to test the plausibility of using stereological sampling for fecundity on histological samples of white perch ovarian tissue. Fecundity sampling was performed on fish from two Chesapeake Bay tributary populations, as well as a geographically isolated control. Data showed substantial agreement between the two methods, both of which produced results within other reported ranges for white perch fecundity indicating validity of added automation. Adding automation also yielded improvements in sampling efficiency, reducing sampling time by 97% for gravimetric counting methods.

2.2 Introduction

Fecundity, or the number of viable oocytes per individual, per spawning cycle, is an important metric in the study of population viability and production in stock assessments, and can be studied using a number of different methodologies depending

on reproductive strategy. Typically, metrics such as recruitment indices and spawning stock biomass (SSB) are used to estimate population levels in fish due to their relative accuracy despite limited data requirements. Such stock assessment methods, while often useful in determining sustainable yields, are not designed to predict subtle changes in reproductive health, changes which might be contributing factors to population declines or reductions in overall fitness (Murua et al. 2003, Lambert 2008, Saborido-Rey and Trippel 2013). Many teleost species are highly fecund, but enumeration of oocytes often overlooks many important data, including gamete quality, levels of premature atresia, and presence of intersex (Blazer 2002, Blazer et al. 2013). Production of viable gametes, specifically viable oocytes, is an important health metric to consider when determining reproductive potential and identifying population-wide effects of anthropogenic or pathogenic influences.

Of the numerous fecundity sampling methodologies currently and historically used, gravimetric methods are the most commonly utilized, as the equipment required and preparation of oocytes for counting are both minimal (Murua et al. 2013). Gravimetric fecundity calculation relies on enumerating the density of oocytes in a known weight (Murua et al. 2003). The benefit of gravimetric methods lies in the ability to use fresh whole tissue, which can either be enumerated manually with an ocular micrometer and dissecting microscope or any combination of imagery and image analysis available, making sampling comparatively low-cost (Murua et al. 2003, Klibansky and Juanes 2008).

As with gravimetric methods, stereometric methods of fecundity sampling have also seen a resurgence of usage thanks to advances in stereological sampling technology (Murua et al. 2003). Stereological fecundity sampling methods for fish

were developed by Emerson et al. (1990), adapting stereometric principles used for counting lung alveoli developed by Weibel and Gomez (1962), in which the partial area and number of objects is measured and then converted to number of objects per unit volume. One of the principle advantages of using stereological methods is the ability to simultaneously investigate reproductive health and fecundity. Depending on reproductive strategy of target species, fecundity sampling will often involve a histological component, in order to determine oocyte sizes at different developmental stages. Additionally, histological investigations can determine levels of atresia or oocyte resorption, and monitor for intersex. In many instances, blocks of embedded tissues are saved for re-analysis, allowing for sampling of archival tissues and analysis of change over time.

One of the principle drawbacks of most methods of fish fecundity sampling is the time consuming and difficult nature of counting small, highly abundant oocytes, but advances in computing technology have provided a number of automated tools, allowing for increased efficiency and larger sample sizes. Previously, automation of oocyte counts was limited to automated particle counting equipment. While automated particle counting has proven highly efficient at sampling fish fecundity, many fish research laboratories, specifically those of management agencies do not have the required equipment (Klibansky and Juanes 2008). Automation of image analysis can eliminate the need for expensive particle counting equipment, while still providing the efficiency of automation. Benefits of using image analysis further include the ability for raw data storage, which can be perpetually re-analyzed if saved (Friedland et al. 2005). Automated or semi-automated image analysis for gravimetric fecundity sampling has been utilized on a number of species, including Dover sole

Solea solea, Southern kingfish *Menticirrhus americanus* and Atlantic cod *Gadus morhua* with reasonable results when compared to other methodologies (Thorsen and Kjesbu 2001, Witthames 2003, Ganias et al. 2010). Stereological fecundity sampling has also benefitted from recent increases in availability of open-source analysis programs. ImageJ (version 1.47; National Institutes of Health, Bethesda, Maryland) and novel programs such as Govocitos (CSIC, Madrid, Spain) have been specifically used to calculate fish fecundity from histological samples where analysis of fresh samples was not possible (Ganias et al. 2010, Costa et al. 2016, Pintor et al. 2016).

White perch in the Chesapeake Bay present an interesting case study to experiment with partial automation of both gravimetric and stereological fecundity sampling procedures, and were selected because of management interest in updating fecundity data in the region. White perch are highly studied in the Chesapeake Bay region due to their relative abundance and ubiquitous presence in all estuarine habitats (Setzler-Hamilton 1991, Kraus and Secor 2004, Kerr et al. 2009). A highly fecund species, white perch total egg production ranges from 5,000 to 300,000 oocytes per ovary in some locations (Setzler-Hamilton 1991).

Most studies on white perch fecundity have focused on simple counts performed gravimetrically or volumetrically (Klauda et al. 1988, Setzler-Hamilton 1991, Okoye et al. 2008). Stereological fecundity methods have yet to be tested on white perch, but if effective, could prove useful at estimating fecundity while simultaneously allowing for histological examination of oocyte quality, intersex, and atresia rates, all of which can provide important information on individual reproductive health. Given that gravimetric methods are typically the benchmark for most fecundity studies, stereological methods will be compared against gravimetric

data to determine efficacy of using stereological methods (Emerson et al. 1990, Cooper et al. 2005, Murua et al. 2003). If methods are acceptable in terms of precision, they will prove useful in answering questions on reproductive output desired by management agencies but, could also provide new management tools for the monitoring of reproductive health in white perch populations.

2.3 Methods

2.3.1 Field Collections

Field collections for fecundity focused on pre-spawn fish in the Choptank, Severn Rivers (Figure 3.1), both tributaries of the Maryland portion of the Chesapeake Bay. Timing of field sampling was determined from observed temporal patterns of white perch spawning activity in each tributary and ongoing field assessments of overall spawning condition of the target population (Table 2.1). Spawning condition was checked at the time of collection using the expression method, which relies on noting the ease of gamete expression from the gonadal vent with manual palpation (Mansueti 1961, Schreck and Moyle 1990). Fish that are closer to spawning condition, or "running ripe", will require less pressure to express gametes, with actively spawning fish requiring little to no pressure (Mansueti 1961).

Fyke nets were deployed in the Choptank and Severn Rivers to capture fish moving to upriver spawning grounds. Fyke nets were set perpendicular to shore with a combination of a parallel lead line extending into the river and "wings" set at a 45° angle from the lead to direct swimming fish into the interior net. Net mesh was 64 mm nylon for net bodies and 76 mm nylon mesh for lead lines and wings (Piavis and Webb 2017). Nets were checked and emptied every 24 hours to minimize stress of

captured fish. A separate set of 20 geographically discrete samples were collected from the Saluda River, South Carolina using electrofishing techniques. South Carolina samples were used as a geographically-isolated control to ensure methods were not only salient for Chesapeake Bay populations. As specimens sampled for fecundity were part of a larger health study, length criteria for collection were used to control for age effects on cumulative lesions, using a total length range of 180 to 240 mm. For fecundity sampling, 180 mm of total fish length also ensures fish had reached sexual maturity. Following capture, fish were transported live without sedation using sealed tanks and supplemental oxygen.

2.3.2 Necropsy

Necropsy examinations were performed at the NOAA Cooperative Oxford Lab (Oxford, MD). Specimens were euthanized in a buffered solution of Tricaine methanesulfate (Tricaine-S MS-222, Syndel, Ferndale, WA) and sodium bicarbonate ($NaHCO_3$), as per MDNR animal use protocols and following the guidelines for the treatment of fish by the American Fisheries Society (USFWS and AFS-FHS, 2014). Morphometric data collected included total weight, eviscerated weight, and total length. Internal examination involved opening the abdominal cavity with an incision from the anal vent to the operculum. Organs were examined for gross pathology, with spleen, liver and gonad excised and individually weighed (±0.0001g) for the calculation of somatic indices. The gonadosomatic index (GSI), hepatosomatic index (HSI), splenosomatic index (SSI) were calculated using the same formula for each, as follows:

$$Somatic\ index = \frac{Organ\ weight}{Total\ fish\ weight} \times 100 \qquad \text{(Equation 2.1).}$$

Fish were aged using otolith annuli counting procedures commonly used for stock assessments (Schreck and Moyle 1990). Otoliths were excised and immersed whole (without grinding) in glycerol, where annuli were counted using a dissecting microscope (Webb 2018). Year-class determinations used conventions outlined by MDNR, which considers the start of annulus formation as opposed to calendar years (Webb 2018).

2.3.3 Gravimetric Fecundity Estimation

Fecundity estimates were obtained on pre-spawn white perch, using the gravimetric method with the addition of automated image analysis. Spawning state was estimated by identifying the most prevalent oocyte state (Jackson and Sullivan 1995).

Gravimetric methods use density of oocytes to estimate total number of eggs in an ovary. Estimation is performed by counting the number of oocytes "*n"* in a known weight of ovarian tissue "*w"* and multiplying this by the total weight of the ovary *W* (Equation 2.2; Hunter et al. 1989, Cooper et al. 2005, Murua et al. 2003).

$$F_{EST} = \frac{W}{w} n \qquad \text{(Equation 2.2).}$$

Typically counts are bounded by a certain oocyte size-range based on their vitellogenic state, which varies by species (Murua et al. 2003). Procedurally, ovaries were first excised from each specimen and weighed to calculate GSI. Following the GSI calculation, each ovary was placed in 10% neutral buffered formalin at a ratio of 1:10 tissue to fixative for at least 24 hours. Following fixation ovaries were re-weighed, to account for tissue change resulting from fixation. Duplicate 1.0g (± 0.001g) aliquots were sub-sampled from fixed ovaries and placed in vials of 70%

ethyl alcohol (ETOH) for storage until counting. Aliquots constituted oocytes from both ovarian lobes, sampled from anterior, middle, and posterior sections to alleviate any potential bias of irregular oocyte distribution (Figure 2.1). In addition to aliquots for gravimetric sampling, subsamples of each ovary were taken for histological processing, using the same sampling procedure (Figure 2.1).

Preparation for oocyte counting required separating individual oocytes from connective tissue through a series of rinsing and vortexing procedures. Aliquots were first individually rinsed through an upper sieve (1000 μm) into a lower sieve (10 μm), which collected viable oocytes. Gentle mechanical means of separation using hand tools were employed in the upper sieve to further separate oocytes not immediately separated by water flow. Separated oocytes gathered in the lower sieve were collected and placed in a small vial containing 70% ethyl alcohol where they were vortexed for 15 seconds at 1000 rpm to reduce clumping of oocytes before storage. To ensure oocyte loss did not appreciably occur between sampling and rinsing, storage vials with alcohol were weighed without tissue and then with tissue to ensure aliquot weights did not differ more than 0.01g. Sieves were inverted, rinsed, and scrubbed to ensure any residual oocytes were removed before processing the next sample.

The primary means of counting eggs involved macroscopic imagery as opposed to *in situ* counting with an ocular micrometer. For imagery, oocytes were removed from vials, blotted dry, and loaded into a standard petri dish (100mm diameter) that had been painted black. A thin film of water was introduced to the dish to ensure further oocyte separation but was not to be deeper than one maximum oocyte diameter, a level that was indicated on the side of the dish. Images were taken

on a Nikon D5100 with an AF Micro Nikkor 60 mm lens (Nikon USA, Melville, NY). The camera was mounted on a stand, and positioned 48 cm from the stand base. Photos were 300×300 dpi, and were imported into ImageJ software for analysis. Photos were taken using a flash module with exposure compensation to reduce glare. Before software analysis of any photograph was performed, the global scale was set in ImageJ software to 33.2005 pixels/1.00 mm. Scale was determined by photographing a metric ruler and measuring a known distance using built-in measurement tools in the software. Analysis workflow is as follows: In ImageJ, change the image quality to 8 bit gray-scale, adjust image threshold to highlight oocytes, use the "watershed" tool to separate individual particles automatically based on circularity parameters, analyze particles to automatically count and record number and size of particles (Figure 2.2, Boyd 2011, Brown 2017). Despite efforts to minimize clumping of oocytes in the above sampling procedures, they would occasionally adhere, resulting in larger than possible oocytes (>1.0mm diameter) for white perch. Clumps that were not separated by the "watershed" tool in ImageJ were split using calculations in RStudio (version 1.2.1335, RStudio Inc., Boston, MA). Oocytes that were larger than the 95th quartile of the size frequency distribution were considered clumps of multiple oocytes (Brown 2017). The area of these clumps was divided by mean particle area, yielding an estimate of how many oocytes constituted the clump in question. Accuracy of the separation calculations was verified by inspecting raw photographs using manual counts.

2.3.4 Stereological Fecundity Estimation

Following sub-sampling of ovaries for gravimetric fecundity procedures, ovaries were subsampled sequentially from anterior to posterior for histological

analysis, with full cross-sections placed in cassettes for paraffin embedding (Figure 2.1). Sectioning was performed with a fixed, multi-blade knife with spacing set to 4 mm between blades. To protect against multiple counting of the same structure, sections chosen for histological processing were not adjacent (Figure 2.1).

Tissues were prepared for stereological analysis using standard paraffin embedding methods, wherein hydrated tissues were chemically desiccated and filled with paraffin wax (McCollough 2019). Once embedded, tissues were sectioned on a microtome at 5 μm, stained with a Meyers Hematoxylin-eosin stain, and mounted with coverslips for protection in storage. Stereometric methods followed those of Weibel and Gomez (1962), adapted to fish oocyte counting by Emerson et al. (1990). The method involves counting cross-sections of oocytes within a partial area of ovarian tissue using an overlaid grid on the two-dimensional slide surface, and converting these counts to unit volume through the use of linear calculations (Figure 2.4). The unit area correlates to the size of the sampling grid, which is equivalent to a volume of the same size according to the Delesse Principle as applied to stereology (Weibel and Gomez 1962). The number of oocytes per unit volume was calculated using the formula,

$$N_v = \frac{k}{\beta} \frac{N_a^{3/2}}{V_i^{1/2}} \qquad \text{(Equation 2.3)}$$

where N_a is the number of oocytes per unit area, V_i is the partial volume of oocytes per unit area, k is a size distribution coefficient, and β is a shape coefficient, calculated as the ratio of longest and shortest particle diameter (Emerson et al. 1990, Cooper et al. 2005, Murua et al. 2003).

Size distribution and shape coefficients were necessary to correct for bias in the counts caused by increased abundance of any one stage of oocyte, for example, a lower fecundity due to increased presence of larger vitellogenic oocytes. For more detail on calculations consult Emerson et al., (1990). Following the calculations of N_v, the number of oocytes per ovary can then be calculated by multiplying N_v by the number of volume units in the total volume of the ovary (Equation 2.4).

$$F_{EST} = N_v \times \left(\frac{V_{Ovary}}{n_{unit\ volumes}}\right) \quad \text{(Equation 2.4)}$$

For species with two ovarian lobes, such as white perch, this value must be multiplied by 2.

Counts were performed visually at 4x magnification, using cellSens software (Version 1.13; Olympus America, Inc., Waltham, Massachusetts), which connected directly in real time with an Olympus DP26 microscope camera, fixed to an Olympus BX51 microscope. The starting location for each specimen was selected at one of the four corners of the slide mount using random number generation. Subsequent fields moved in an "S" pattern from top-bottom or bottom-top, using visual inspection and microscope stage measurements to ensure no overlap between sections occurred. Instead of using the typical Weibel multi-purpose grid used by Emerson et al. (1990), a standard grid was employed, as cellSens software did not have Weibel counting capabilities (Figure 2.4). Certain ImageJ plugins exist for such operations, but in order to make the procedure more accessible to managers and field biologists, only base versions of ImageJ software were used with manual counting procedures. The grid field was sized 3000 x 3000 μm with 10 intersections per line (Figure 2.4). Magnification was 4x to facilitate synchronized spawning state identification and fecundity estimation. In order to determine efficacy of using a standard grid,

observational error rates were calculated using established stereological principles (West 2012). Error rates for both number and density data were maintained below 10%. The number of fields required for accurate estimates was deemed to be a minimum of 10 per fish through investigations of observational CV in pilot studies (Shaner unpublished data).

While previous stereometric fecundity studies found it plausible to use average values for the above coefficients k and β, pilot studies of methods with white perch determined that CV values between fish were too great to use average measurements, thereby necessitating calculation for each sample. Calculation of coefficients was automated using both ImageJ software and RStudio for particle analysis and mathematical operations respectively. Images were taken for each sample at 4x magnification using the capture tool in cellSens. Each image was then loaded from a chosen file directory in ImageJ, converted to an 8-bit grayscale image, adjusted for threshold to highlight oocytes, and then analyzed for particle size and diameter. Limits for circularity and maximum particle diameter were determined visually based on trial and error. Minimal *in situ* editing was required to ensure cellular debris, camera glare, and reflections were not included in particle counts, but otherwise the procedure was automated using ImageJ macros. Approximately 20 oocytes were necessary for accurate calculation based on CV investigations (Figure 2.5).

As stereological methods yield volume-based fecundity estimations, volume must be calculated for ovaries in order to estimate fecundity. Volumes were estimated using a wet-weight method, which involves weighing a known volume of water, and then suspending the organ in the quantity of water and noting the change

in weight (Scherle 1970). As ovaries are denser than water, their weight is supported by the apparatus and change in weight on the balance is equivalent to the volume of the organ (Scherle 1970).

2.3.5 Statistical Analysis

Statistical analysis was performed using Microsoft Excel (2016 edition, Microsoft, Redmond, WA) and RStudio. In order to assess the plausibility of using the stereological method on histologically preserved white perch samples, the stereological method was compared with the gravimetric counts from the 2018 sampling season. To determine method precision, replicate counts were performed on 5 white perch using each estimation method. Data from 3 replicate counts of 5 randomly selected specimens for both methods were used to calculate mean, standard deviation (SD), and coefficient of variation (CV). CV was calculated by SD divided by the mean of replicate counts × 100. To assess method agreement, observations from both methodologies were plotted on a Bland-Altman plot (Bland and Altman 1984, Giavarina 2015). Deming and Passing-Bablok regressions were performed to corroborate visual inspection of bias. Lin's concordance correlation coefficient was calculated to further analyze agreement between the methods, and was interpreted based on McBride's strength of agreement criteria for correlation analysis (McBride 2005). Lin's concordance correlation coefficient was used as opposed to Pearson's methods as Lin's methodology accounts for error in both methods.

2.4 Results

For methods comparison study, 42 white perch were sampled from 3 river systems in 2018 (Table 2.1). Severn and Choptank Rivers were sampled in the

Chesapeake Bay, with additional samples from a geographically discrete population from the Saluda River, South Carolina, USA, to test parsimony of methods. Before comparing the two methods against each other, precision was checked for each independently. Automated gravimetric methods averaged a CV of 2.9 for the 5 randomly selected samples, indicating good precision. Stereological methods averaged a CV value of 7.3 for the 5 randomly selected samples. Stereological methods precision was further evaluated for observational error as per methods provided by West (2012), as described in Appendix I.

Bland-Altman plots showed 95% of data points falling between ±1.96 SD confidence intervals as recommended, with no visual indication of constant bias between methods (Figure 2.6; Bland and Altman 1984, Giavarina 2015). Results of the statistical analyses of the methods comparison are summarized in Table 2.2. Correlation between the methods according to Lin's concordance correlation coefficient (CCC) was 0.98, indicating "substantial" agreement between the methods as described by the McBride scale, where CCC values of 0.95 to 0.99 are deemed substantial in practice (McBride 2005). Passing-Bablok and Deming regression did not indicate bias between the stereological and gravimetric methods, corroborating visual inspection of Bland-Altman plots (Table 2.2).

2.5 Discussion

2.5.1 Gravimetric Methods Performance

Fecundity estimates determined with gravimetric sampling methods for Maryland white perch populations in Severn and Choptank Rivers appear in agreement with estimates from other studies on white perch from the Chesapeake and

other watersheds, indicating satisfactory, though qualitative, accuracy of methods. Estimates for fecundity are close to those reported by Mansueti (1961) of 50000 to 150000, indicating possible agreement between current and historical methods used in the Chesapeake Bay. However, it is impossible to determine actual agreement, as methods from the original study were not reported (Mansueti 1961).

Based on *in situ* ground-truthing of results and agreement with reported white perch fecundity ranges from other studies, the addition of automated particle counting did not appear to adversely impact sampling accuracy while increasing sampling efficiency. Regarding efficiency, the automated counting methods were an improvement to simple ocular counting. The 129 samples analyzed using automated gravimetric sampling, were counted for fecundity in approximately 40 hours. Given this rate of sampling, automated gravimetric fecundity could be used to rapidly develop fecundity databases to allow for monitoring of fecundity over time, which is often lacking for many species (Saborido-Rey and Trippel 2013). This increased efficiency would also enable larger sample sizes to be used for population estimates of fecundity, thereby improving precision. For instance, previous studies dealt with relatively small sample sizes, including sample sizes of 10, 50, and 34 in studies on the Quabbin Reservoir, Massachusetts, USA, Lake Erie, and the Wagon Train Reservoir in Nebraska, USA, respectively, but were deemed representative of population levels (Taub 1969, Zuerlein 1981, Bur 1986).

Automation of gravimetric sampling methods also increases the accuracy of counting particles of different size classes. For species, such as white perch, which are asynchronous or group-synchronous and have multiple clutches of eggs in different stages of development present each spawning season, it is important to

ensure that only those oocytes that are sufficiently developed for spawning are counted, meaning eggs over 0.2 mm in diameter (Klauda et al. 1988, Jackson and Sullivan 1995). While this can be done through mechanical means, such as using specific mesh sizes of sieves to capture or exclude certain size classes of oocytes, software is able to differentiate size classes accurately and instantly.

2.5.2 Stereological methods performance

The primary impetus for undertaking a methods comparison was to evaluate the efficiency of the two methods and determine if the more expedient technique was adequate for management purposes. A secondary point was to evaluate if the methods could appropriately be used to determine fecundity in archived histological samples. As white perch are a new species for stereological fecundity methods, high values of Lin's concordance correlation coefficient, and lack of bias as shown by Passing-Bablok and Deming regression analysis and Bland Altman plotting methods (Figure 2.8) when comparing stereological and gravimetric methods, show the salience of the stereological method's usage. Thus, adding stereological methods to the tools available for white perch fecundity sampling allows for analysis of other archival histological samples in collections throughout the white perch geographical range. Care, however, must be practiced in determining the source of the histological sections in the ovarian tissue, as contiguous sections placed on the same microscope slide will result in double counting. It is uncertain whether such methodologies would be valid for dissector-style histological sampling.

The methods used in this study to stereologically estimate white perch fecundity differed in key ways from other stereological studies, notably in the calculation of coefficients used to correct for differences in oocyte size distributions

and oocyte shape between individuals and the number of fields used for estimates. Original stereological fecundity methods formulated by Emerson et al. (1990) called for the calculation of the size distribution coefficient "k" for each specimen, and using an average value determined in pilot studies for the shape coefficient β. For this study, variations of coefficient values between specimens in pilot studies were large enough in magnitude (Figure 2.5) to merit calculation for each specimen separately (Emerson et al. 1990). Other more recent stereological studies used constant values for both coefficients including studies on shortspine thornyhead *Sebastolobus alascanus*, longfinger anchovy *Anchoa filifera*, and Southern kingfish *Menticirrhus americanus* (Cooper et al. 2005, Costa et al. 2016). Use of such average values could possibly impact accuracy of fecundity data, but agreement between the methods in other comparative studies indicate no noticeable impact of using average values for coefficients (Emerson et al. 1990, Cooper et al. 2005). Fluctuations in coefficient values for white perch are possibly due to their asynchronous development but could also be the result of small sample sizes.

Another notable deviation from other stereological studies is that the number of grids counted per specimen required for this study were appreciably lower than previous studies on species of similar ovarian volume. The original study of Emerson et al. (1990) used between 15 and 20 counts per specimen regardless of species, and subsequent studies on *S. alascanus* and *M. americanus* used an average of 55 and 22 counts per specimen respectively (Costa et al. 2016). This number of grid counts stands in contrast to the observed minimum of 10 fields for white perch in this study, based on pilot study in observational error. Investigating number of counts per fish was undertaken for this study to find a balance between observed error and sampling

efficiency but also because histological tissue samples from MDNR health studies used in this study often did not have enough tissue to support the 20 distinct fields called for by Emerson et al. (1990). Investigations of observational error (Appendix I), and investigation of CV of fecundity estimates indicated that, while 15-20 counts would provide more precision, counts of 10 were sufficient to maintain observational error below the accepted 10%. Were methods to be used on archival samples in other collections, investigations into the efficacy of using 8 to 10 fields would need to be undertaken prior to study, as per observational error investigations in Appendix I.

Despite gravimetric methods being the accepted methodology for most fecundity studies, whole oocyte counting methods, such as the gravimetric procedures, still require histological sampling to ensure specimens are sexually mature and also have not begun ovulation (Murua et al. 2003). For the determination of spawning state alone, histology is of critical importance, because field-based methods for determining spawning state are fairly crude. As was the case with this study, properly vetting the samples used, through histological oocyte staging, enabled the elimination of a number of actively spawning individuals, specifically from originally included sampling sites on the Lower Susquehanna River and Loch Raven Reservoir (Patapsco River, Baltimore, MD), whose inclusion would have putatively altered results.

For stereological methods in particular, the argument could be made that methods are antiquated given the now widespread availability of image analysis software and equipment used for photographing and analyzing aliquots of whole oocytes. However, the demonstrated need for histological analysis, even with whole oocyte counting methods, keeps stereological methods relevant. Advantages of the

stereological method include the ability to simultaneously determine oocyte developmental state and sample fecundity, as well as monitor for reproductive health pathology such as intersex and atresia. Atresia is especially important considering its relationship with environmental stress (Barton et al. 2002, Schreck et al. 2001). Given the abundance and trophic importance of white perch in the estuaries of the Eastern United States, the demonstrated utility of both fecundity sampling methods used in this study will allow for more research into the impacts of anthropogenic drivers on reproductive success, in order to better manage future change.

2.6 Tables and Figures

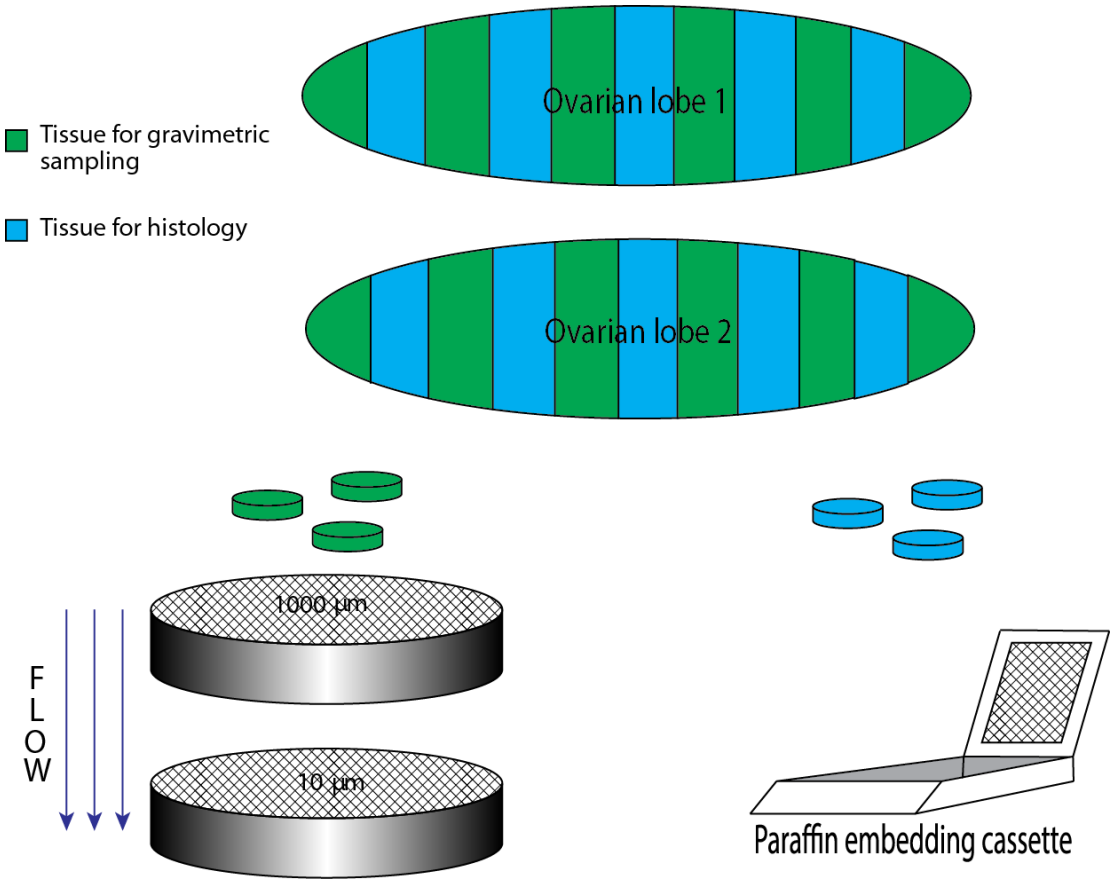

Figure 2.1 Histological sampling procedure used for collection of tissues for white perch fecundity estimation. In 2018, ovaries were used for both gravimetric and stereological sampling methods as indicated. For all other years, only histological tissues were taken.

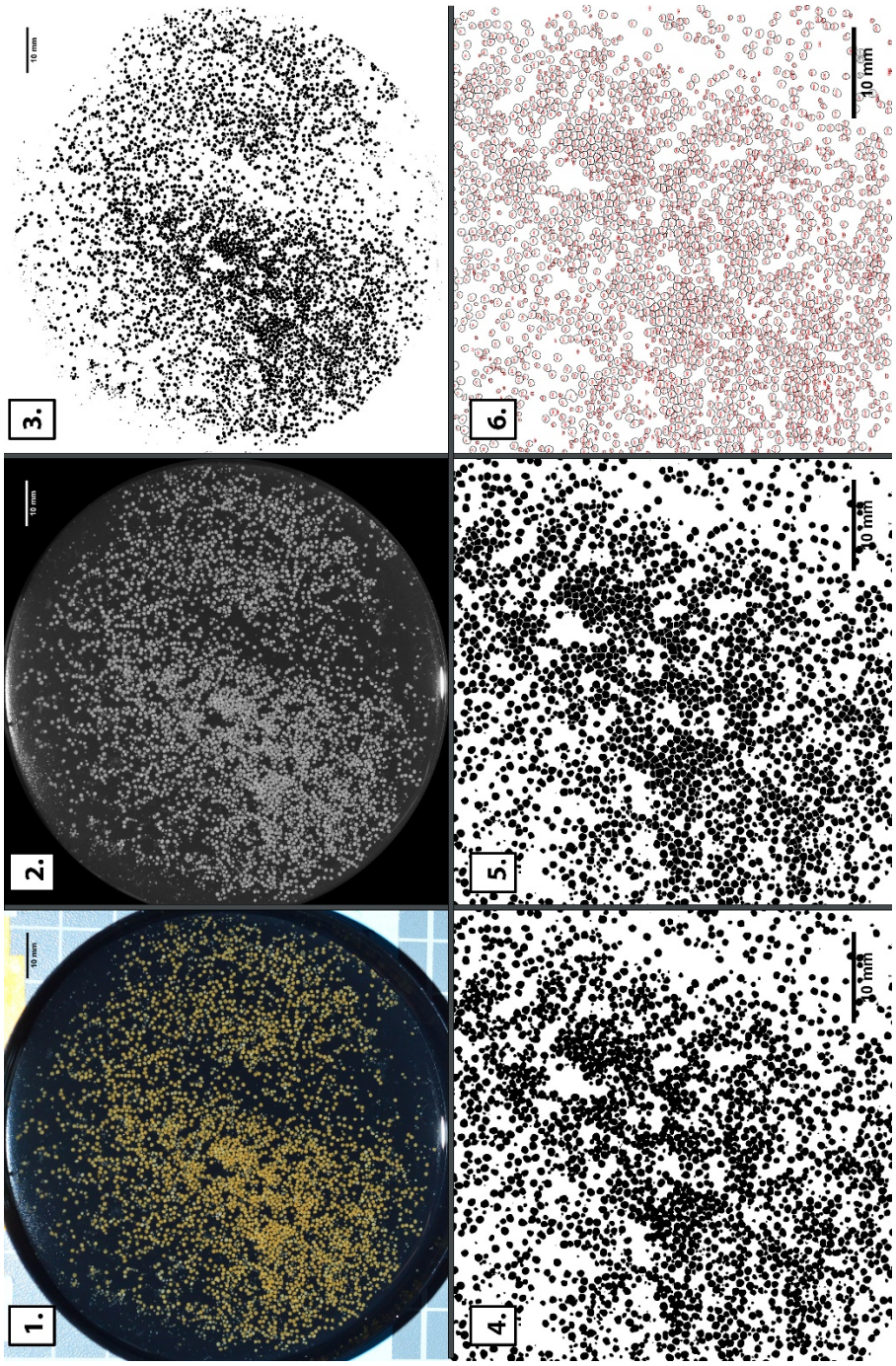

Figure 2.2 Typical automated gravimetric fecundity sampling workflow for image analysis of white perch oocytes in ImageJ. Scale bars = 10 µm **1.** Original image, **2.** Adjusted to 8-bit grayscale, and background removed, **3.** Thresholding of image to highlight oocytes, **4.** Zoomed version of panel 3 showing some oocytes sharing common borders (clumps), **5.** "Watershed" procedure, where according to circularity parameters software separates distinct particles, **6.** Counted, numbered individual particles. With the exception of limited editing to remove glare in panel 3, all processes were automated by macro programing.

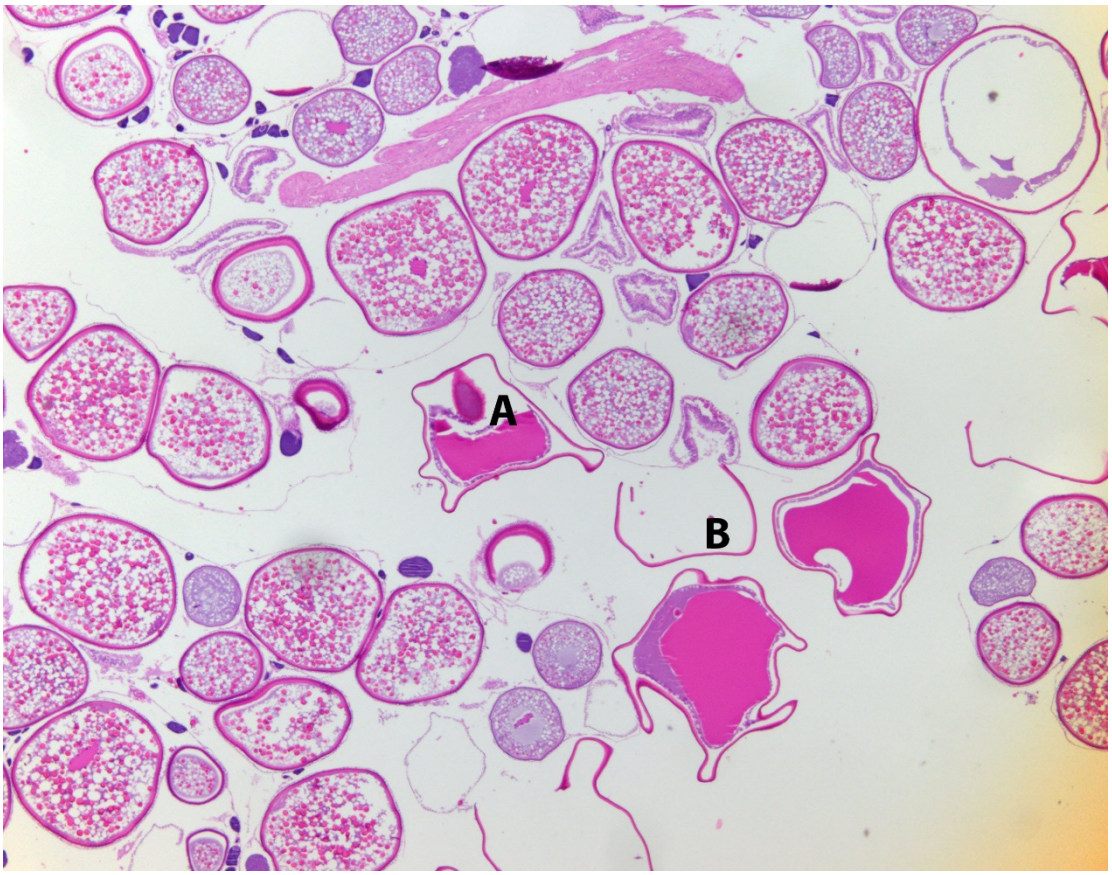

Figure 2.3 Example of a white perch specimen that has commenced ovulation, shown at 4x magnification. Signs of ovulation include **A.** increased atresia and the presence of **B.** shed chorion membranes. Samples which exhibited any similar signs were removed from analysis.

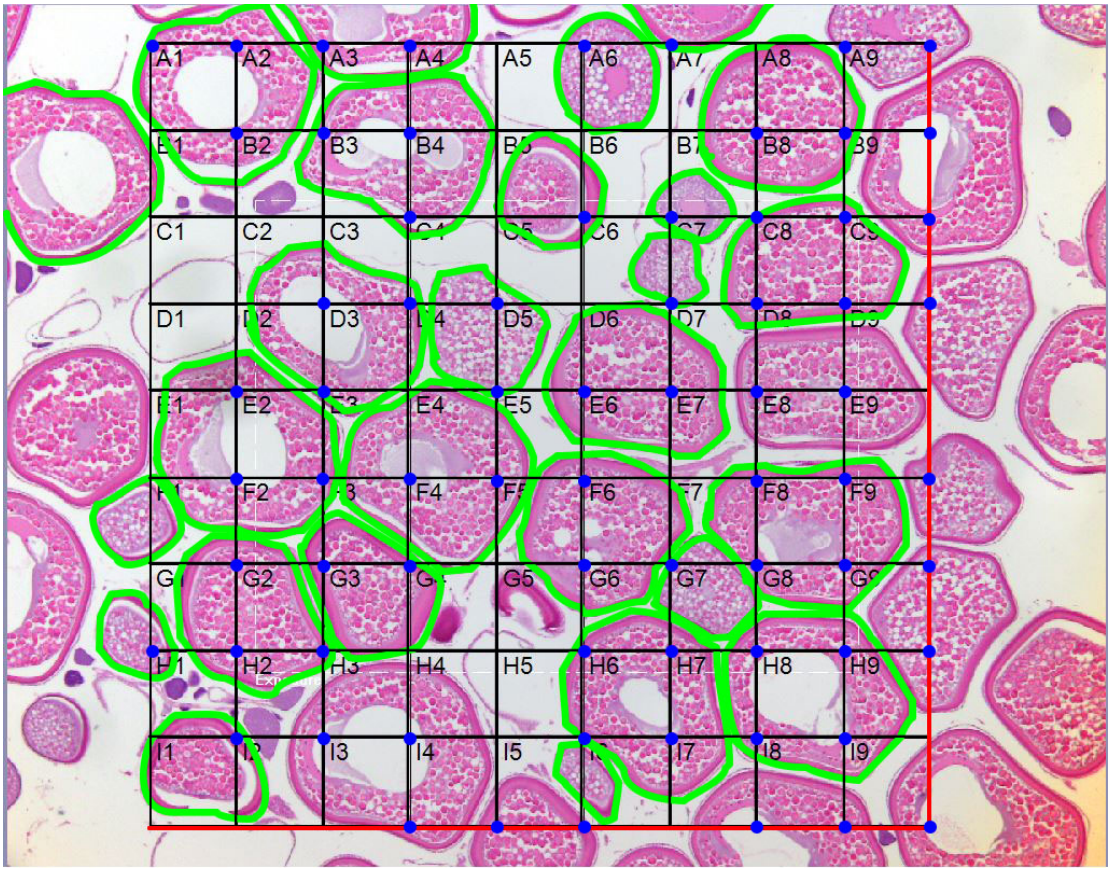

Figure 2.4 Image of a typical sampling field grid from stereological fecundity investigations of white perch. Image at 4x magnification, with a grid of 3000 μm^2. Partial area of oocytes per field is determined by number of grid intersections lying over oocytes. For this field, P=71 points, indicated by blue dots, that yields a partial area of 0.71×grid area. Number of oocytes are the number of oocytes partially or totally falling within the grid. For this field, N=27 whole oocytes, which are highlighted in green. Oocytes which intersected the right and bottom grid borders were not counted by convention.

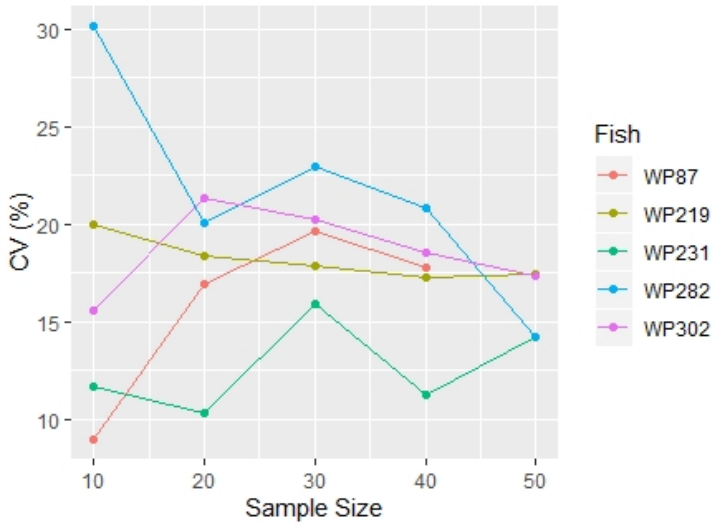

Figure 2.5 CV calculations to determine number of oocytes required of white perch samples to accurately calculate shape and size distribution coefficients used in stereological fecundity calculations. Five fish from multiple sampling locations were selected, with estimates determined by randomly selecting a specified number of fecundity particle results to complete calculations based on random number ordering in Microsoft Excel.

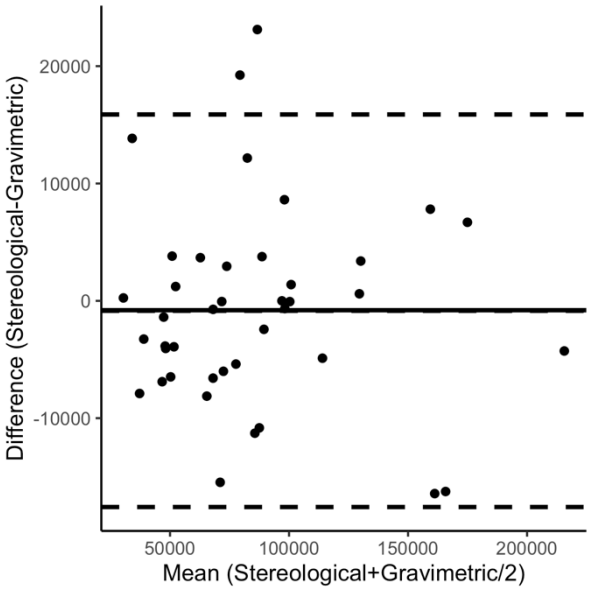

Figure 2.6 Bland-Altman plot comparing gravimetric and stereological methods when used on white perch. Confidence intervals are ±1.96 SD, indicated by dashed lines. Solid line indicates the mean of the differences between the two methods.

Table 2.1 Locations sampled and number of white perch specimens used for both gravimetric and stereological methods of fecundity sampling in 2018.

Sampling Location	*Sampling dates (2018)*	*Temp (°C)*	*Salinity (psu)*	*Specimens (Gravimetric)*	*Specimens (Stereological)*
Choptank River	27-Feb	10.15	0.11	6	0
	13-Mar to 15-Mar	5.89	0.28	30	0
	28 Mar to 29 Mar	7.37	0.28	30	9
Severn River	19-Mar	5.79	10.07	4	0
	26-Mar	7.85	9.63	26	0
	17-Apr	14.15	8.46	13	13
Saluda River (SC)	30-Mar	NA	NA	20	20
TOTALS				129	42

Table 2.2 Results of Lin's concordance correlation coefficient and Deming and Passing-Bablok Regression for comparison of stereological and gravimetric fecundity sampling methods. Confidence intervals are indicated in parentheses. Intervals contain 0 for both intercepts, and 1 for both slopes, indicating no statistical evidence of bias.

	Lin's CCC	Deming Regression	Passing-Bablok Regression
Stereological vs. Gravimetric methods	0.979	**Intercept**: –107.91 (–5786.51 - 5583.98) **Slope**: 1.01 (0.94 - 1.07)	**Intercept**: –2717.75 (–9081.37 - 2745.47) **Slope**: 1.02 (0.95 - 1.10)

Chapter 3: Investigations of effects of multiple stressors on the reproductive health of White Perch (*Morone americana*) in select Chesapeake Bay tributaries

3.1 Abstract

White perch are a highly fecund species with small home ranges, making them good candidates for comparative ecosystem health studies. While recruitment of white perch sub-populations in the Chesapeake Bay has not shown indications of reproductive failure, modeling of fecundity could increase the sensitivity of spawning stock metrics. This study seeks to model possible connections between environmental degradation and reproduction in white perch but to also identify influences on individual fecundity such as disease loading and body condition. Sub-population fecundity in the Severn and Choptank Rivers was estimated using stereological and gravimetric fecundity sampling methods. Comparisons of riverine populations yielded no conclusive evidence of anthropogenic influence on fecundity. On an individual level, variation in fecundity was unaffected by disease covariates and only affected in a limited capacity by nutrition, with fish weight found to be the most influential factor on fecundity. As white perch fecundity has not been modeled over time until this study, methods present opportunity for further expansion of the body of work, to include study of oocyte quality and impacts of climate.

3.2 Introduction

Reproductive output of marine fish has become an important area of study, striving to not only provide more detail on energy partitioning and individual health, but also to provide more detailed information on recruitment or, in some cases, explain a chronic lack of recovery in exploited stocks (Lambert 2008, Sabordido-Rey

and Trippel 2013). While metrics of population abundance and reproduction such as spawning stock biomass (SSB) provide important information, adding information on variations in egg production, or fecundity, can provide a more complete picture of stock production and recruitment (Sabordido-Rey and Trippel 2013). Use of fecundity data for fisheries management, however, can prove challenging with species that exhibit non-uniform reproductive strategies, including presence of oocytes in multiple stages of development while spawning, or the ability to forgo spawning in a given year.

Understanding potential drivers of fecundity variation, including nutrition, disease, and habitat quality, is a first step in the understanding of why recruitment fluctuates and how that may affect management decisions. Fecundity in many species has been shown to change in response to a number of factors, including health, nutritional state, and ambient water quality (Schreck et al. 2001, Kavanagh et al. 2004, Tanaka et al. 2017). Better understanding the drivers of fecundity fluctuation can provide important information for use in management, specifically in the face of climate shifts or changes in fishing pressure.

The interest of Maryland Department of Natural Resources (MDNR) fisheries managers in the reproductive health and output of white perch in the Upper Chesapeake Bay presents an opportunity to further the understanding of reproduction in asynchronous spawners, and also use on-going health surveys to model fecundity against pathological, environmental, and nutritional covariates. While recruitment indices and population abundance estimates for white perch in the Chesapeake Bay continue to show increasing trends, fecundity in white perch has not been investigated

in the Chesapeake region since the early 1960s (Mansueti 1961, Piavis and Webb 2017).

Reasons for modeling fecundity of white perch with respect to habitat quality and disease, is based in a large body of work linking anthropogenic influences in the form of contamination, nutrient pollution leading to hypoxic conditions, and pathogen introductions, to lower individual fitness in many fish species (Adams et al. 1993, 1996, Barton et al. 2002, Greeley 2002, Iwanowicz 2011, Uphoff et al. 2011). Evidence exists in many fish species of the Chesapeake Bay region of subtle reproductive effects of anthropogenically-driven contamination, such as intersex and tumor prevalence (Kavanagh et al. 2004, Pinkney et al. 2011, Blazer et al. 2013, 2014). Specifically, species such as Yellow perch *Perca flavescens*, Brown bullhead catfish *Ameiurus nebulosus*, and Small *Micropterus dolomieu* and Largemouth bass *Micropterus salmoides* have been shown to be susceptible to anthropogenic influence, specifically in the form of contamination (Pinkney et al. 2011, Blazer et al. 2013, 2014). Effects of environmental contamination range from increased tumor prevalence to outright reproductive failure (Pinkney et al. 2011, Blazer et al. 2013).

Regarding the effects of direct anthropogenic influence on white perch in the Chesapeake Bay specifically, health data collected for use in the MDNR Health Assessment Index (HAI) project were compared to fecundity data for the Severn and Choptank Rivers, Maryland, USA. The HAI functions by quantifying gross pathological observations by sampling location in order to determine if habitat quality is having a quantifiable impact on white perch sub-populations. The index has been used to successfully quantify impacts of environmental degradation on white perch in the Tred Avon River, Maryland (McLaughlin et al. 2018). Perch in the upper portion

of the river, where runoff from urbanized areas has contributed to lower oxygen levels and higher sediment contamination, exhibited significantly greater overall scores in gross pathology indices, and higher indo-parasite burdens than fish in the less impacted, lower river sites (McLaughlin et al. 2018).

In addition to investigations of the direct physiological effects of habitat quality, MDNR included components of mycobacteriosis prevalence and coccidian parasite burden to determine if disease is having a quantifiable impact on reproduction. Pre-disposition to disease can be a secondary effect of habitat-induced stress, with pathogens often exploiting physiologically compromised individuals (Barton et al. 2002, Roberts 2012). White perch in the Chesapeake Bay present disease symptoms similar to those of other species of the region, including granulomatous mycobacteriosis infection, hepatic tumors, and signs of hypoxia-induced stress (MDNR unpublished data). Mycobacteriosis in particular, has been increasing in relevance due to its high prevalence in Chesapeake Bay Striped bass (*M. saxitilis*) populations since 1997 (Jacobs et al. 2009, MDNR unpublished data). Prevalence in resident striped bass is consistently >50%, which stands in contrast to migratory populations, that have observed prevalence of <10% (Matsche et al. 2010).

Anthropogenic influence in the Chesapeake Bay is one hypothesized cause for higher mycobacteriosis prevalence in the Bay population, in that pollution-induced hypoxia results in higher stress levels, as well as a higher environmental burden of mycobacterial species (Kane et al. 2007). The disease effects in striped bass range from granulomatous lesions in splenic tissue to widespread coverage of ulcerative lesions in the dermal surface (Gauthier and Rhodes 2009, Jacobs et al. 2009). Impacts of mycobacteriosis on reproduction and recruitment appear to be more

discrete, with the limited evidence of the infection impacts being muddled by increased mortality and the possibility of fecundity shifts for unrelated reasons (Gervasi et al. 2019).

In addition to striped bass, mycobacteriosis infection has been observed in numerous Chesapeake Bay species including white perch (Kane et al. 2007, Jacobs et al. 2009). Prevalence levels in white perch remain <30%, with only limited related gross pathology, such as visible ulcerative lesions (MDNR, unpublished data). Mycobacteriosis in white perch is typically found through histological examination of splenic tissue due to lack of external pathology. Despite limited gross pathological effects of mycobacteriosis on white perch, the higher infection rate among resident species of the Bay, makes reproductive effects worth investigating.

Given the considerable commercial and recreational use of the Chesapeake Bay, introduced pathogens are also of concern, particularly the novel coccidian parasite infestation recently documented in white perch of the Bay (Matsche et al. 2019a). Coccidian parasitism is an additional stressor that has the potential to exert influence on the reproductive health of white perch, because the primary location of infection is the gallbladder and bile duct. Liver inflammation and necrosis are present in the most virulent cases of observed coccidiosis in white perch, leading to supposition of possible reproductive effects, as the liver is an important producer of lipids and proteins used in egg development (Matsche et al. in press).

In general, the fish species of the Chesapeake Bay are well-studied regarding their individual health, but links from these health data to reproductive output are harder to find. The goal of the present study is to begin to increase the understanding of how drivers such as disease and habitat quality impact reproductive health, using

white perch as a subject because of the large amount of location-specific health data amassed by MDNR studies from 2014-2020. Quantification of links between habitat quality and reproductive health will provide data to fisheries managers as to the impacts of watershed management policies on the resilience of white perch populations to multiple potential reproductive stressors.

3.3 Methods

3.3.1 Field Collections

Field collections of specimens were performed in multiple Maryland riverine populations of white perch during annual spawning from 2015 to 2018. Specimens were captured in fyke nets set above Kingston Landing on the Choptank River from 2015 to 2018 and in Little Round Bay in the Severn River in 2018 in order to sample from the populations during typical spawning migrations. Specimens collected from 2015-2017 were humanely dispatched at time of capture using MDNR animal use protocols and following the guidelines for the treatment of fish by the American Fisheries Society (USFWS and AFS-FHS, 2014). After capture they were transported on ice to the Cooperative Oxford Lab (Oxford, MD) and necropsied. Samples taken in 2018 were transported live in water with supplemental oxygen, before being humanely dispatched as per MDNR animal use protocols (USFWS and AFS-FHS, 2014). Specimens were examined externally for visual signs of trauma or disease, and then opened from the anal vent to the operculum for internal examination.

Quantification of anthropogenic influence on watersheds was performed for the Severn and Choptank River systems using USGS funded water column

contaminants sampling performed in 2018, and watershed land-use characteristics from a high-resolution dataset developed by the Chesapeake Bay Program (2013 high-resolution land use dataset, Chesapeake Bay Program Office, Annapolis, MD). Contaminants sampling utilized passive water sampling techniques, which involved deployment of semi-permeable membrane devices (SPMD) contained in bottom mounted sampling canisters in two locations (one in headwaters, one in tidal waters) per river (Matsche et al. in press). Membranes were analyzed for polycyclic aromatic hydrocarbon (PAH) compounds, organochlorine pesticides, and brominated diphenyl ethers (BDE) (Matsche et al. in press).

3.3.2 Health quantification

Specimens were examined as part of a MDNR Health Assessment Index (HAI) in an effort to determine linkages between anthropogenic influences and population health. Metrics were adapted from those used by Adams et al. (1993), with additional metrics for specific pathogens and hematology added by MDNR. The HAI functions by quantification of gross pathology presence and severity, in order to examine trends in discrete populations. Metrics in the HAI include gross pathological assessment of external and internal lesions, parasite loading, and other abnormalities, such as damage from fishing activities (Table 3.1). Categories were assigned based on major organs both externally and internally, including gills, integument, spleen, and liver (Table 3.1). Scoring was by increments of 10, with mild, moderate, and severe observations receiving scores of 10, 20, and 30 respectively. Multiple conditions in one organ group were summed. For example, a spleen with moderate granuloma prevalence (20 score), and mild parasite prevalence (10 score) would

receive a total score or 30. The total HAI score is a relative measure of gross pathology severity and was obtained by totaling all scores from all categories.

In addition to gross pathology, additional physiological information collected included somatic indices and nutritional indicators, as well as presence and severity of mycobacteriosis infection. Somatic indices were calculated for spleen, liver and gonad, following the formula,

$$Somatic\ index = \frac{Organ\ weight}{Total\ fish\ weight} \times 100 \qquad \text{(Equation 3.1).}$$

Fulton's condition factor and relative amount of internal mesenteric body fat were used as indicators of nutritional state of each specimen. Fulton's condition factor was calculated using total weights from all specimens, using the following formula,

$$K = \frac{W}{L^3} \times 100 \qquad \text{(Equation 3.2)}$$

where K is Fulton's Condition Factor, W is total specimen weight, and L is total specimen length. The Body Fat Index (BFI) is calculated subjectively by necropsy observers and is based on work with striped bass and mycobacteriosis infection (Jacobs et al. 2013). Here the amount of mesenteric body fat is rated on a scale of 0-3, with 0 being no visible fat deposits, and 3 being enough fat to alter external body shape and obscure internal organs from the necropsy technician (Adams et al. 1993, Jacobs et al. 2013).

Mycobacteriosis infection was quantified using established histological techniques, where splenic tissues were sequentially sectioned from anterior to posterior, embedded in paraffin, and stained with an acid-fast stain to highlight active mycobacteria (Matsche et al. 2010). Presence of active bacterial colonies inside granulomas was then quantified by manually scanning slides in a grid pattern at 4x to

observe granulomas and then 10x on specific granulomas to determine presence of mycobacterial colonies.

3.3.3 Fecundity Estimation

Fecundity data for location comparisons were collected using gravimetric methods from fresh samples in 2018 (Cooper et al. 2005, Murua et al. 2003). Ovaries from 109 white perch from the Choptank and Severn Rivers, were excised from specimens, weighed for calculation of gonadosomatic index (GSI), and sampled sequentially from anterior to posterior (Figure 2.1, Table 3.1). Aliquots for gravimetric counting were 1.0g (0.001g) comprised of oocytes from anterior, middle, and posterior ovarian regions. Samples were washed through a 1000 μm mesh sieve using mechanical separation to remove oocytes from connective tissue. Loose oocytes were collected in a 10 μm mesh sieve, placed into weighed vials of 70% ETOH, reweighed to ensure minimal tissue loss and vortexed at 1000 rpm for 15 seconds. Oocytes were spread in the base of a black painted, 10 cm diameter glass petri dish and photographed for counting. Counts were performed using ImageJ, which involved an automated process of image editing and particle analysis (Figure 2.2). Count corrections for oocyte clumps were performed using RStudio analysis (Appendix II).

Specimens used for time series, disease, and water quality effects analysis were from the Choptank River population collected pre-spawn from 2015 to 2018, totaling 182 samples. Fecundity data for these analyses were obtained through stereological methods, as fresh tissue for gravimetric analysis was not available for specimens collected from 2015 to 2017 (Emerson et al. 1990, Murua et al. 2003). A total of 182 histological slide samples of gonad tissue from pre-spawn sampling in the

Choptank River from 2015-2018 were compared by year to determine temporal fecundity variability (Table 3.1). Stereological fecundity estimation required point counting the number of oocytes and area occupied by oocytes in the known area of a sampling grid. Before point counting, the developmental stage of each sample was checked for signs of ovulation using stereoscopic observation (Jackson and Sullivan 1995). Those samples that indicated ovulation had commenced were removed from consideration, as the onset of spawning would skew total fecundity counts, making them inaccurate. Point counts were performed using the cellSens digital ocular designed for Olympus optics, using a digitally superimposed 10×10 standard grid, 3000 μm^2 in size. The number of fields counted per specimen was dictated by the amount of tissue present on each slide, although a required minimum of 10 was necessary to reduce observational error, as was found in pilot studies (Appendix I). Calculations included size distribution and shape coefficients to correct for variations in oocyte size distribution and oocyte shape. Coefficients were determined electronically using photos of each specimen at 4x magnification and ImageJ macro scripts for automation of repetitive procedures (Appendix II), using calculations from Emerson et al. (1990).

As histological ovarian samples from 2015-2018 were not sampled for volume, it was necessary to predict organ volumes for stereological fecundity calculations (Emerson et al. 1990). Organ volume was predicted from organ mass, using a linear model constructed with data from 61 fresh ovarian samples from 2020 for which both mass and wet weight for volume were recorded (Figure 3.2). Samples were collected pre-spawn in 2020 in the Choptank River from fyke nets used for yearly abundance surveys by MDNR. Volumes were estimated using the wet-weight

method, in which the whole ovary was suspended in water, with the difference in weight between the water as weighed before and after organ submersion corresponding to volume (Scherle 1970). The linear model was tested for agreement with assumptions of linearity, independence and normality of errors using RStudio model diagnostics. Following model validation, volumes were predicted from mass data using the following formula,

$V = 0.58110 + 0.96842(M) + 1.233$ (Equation 3.3),

where V is organ volume and M is organ mass.

3.3.4 Statistical Analysis

Modeling of fecundity in response to the effects of sampling location, disease, and individual nutrition, was performed using the information-theoretic approach of model selection with RStudio and Microsoft Excel (2016 edition, Microsoft, Redmond, WA) (Burnham and Anderson 2002, Burnham et al. 2011, Jacobs et al. 2013). Model selection procedures involved creation of a set of candidate models using potential covariates described in literature as having influence on fecundity, along with a null model to determine observational error rates and ensure no collinearity among covariates (Burnham and Anderson 2002, Jacobs et al. 2013). Modeling was performed using generalized linear models of the Guassian family. Models were evaluated based on an adjusted Akaike Information Criterion (AICc), for use with small sample sizes, which ranks models in a candidate set based on their relative distance from the "truth" (Burnham and Anderson 2002). In comparison to the typical use of the un-adjusted AIC, using the AICc creates a more robust estimate of model efficacy, though both measures will eventually converge as a function of sample size (Burnham and Anderson 2002). Using AICc, each model in the set was

evaluated for performance based on the other models in the set, with AICc weights (AIC_w) on a scale of 1-0 being used as a quantitative measure of performance.

$$AIC_w = \frac{e\left(-\frac{1}{2}\times\Delta AICc\right)}{\sum_{r=1}^{R} e\left(-\frac{1}{2}\times\Delta AICc\right)} \quad \text{(Equation 3.4)}$$

The model that performed the best in selection procedures, or had highest AICw, was selected as the best explanatory model, with all other models in the set then compared to that model on a basis of difference in AICc scores (ΔAICc). To compare models for strength of evidence, ΔAICc are used for direct comparisons or are used to calculate model likelihoods ($\mathcal{L}$) which can then be used to calculate probabilities (Equation 3.5).

$$\mathcal{L}_i = \exp\left(-\left(\frac{1}{2}\right)\Delta_i\right) \quad \text{(Equation 3.5)}$$

When comparing ΔAICc scores directly, a scale will be used that generally supports a model with difference >14 as being implausible (Burnham et al. 2011). Likelihood calculations will be used to provide another form of evidence in the form of probabilities, which are calculated simply by dividing the probability of the best model in the set by the likelihood of other models in the set (Burnham et al. 2011).

Before determining the effects of disease, nutrition, and geographic location, a base model was first created from morphometric variables determined to be influential in previous studies, including total length (TL), total weight (TW), and age (A) (Emerson et al. 1990, Cooper et al. 2005, Murua et al. 2003, Costa et al. 2016, Tanaka et al. 2017). To eliminate the possibility of geographic difference between discrete populations, base model selection and testing of other influential factors, was performed solely on the Choptank River sub-population of white perch.

Following the selection of a base model, nutrition, disease, and sampling location parameters were added to investigate their respective influence on fecundity. Model selection procedures and evaluation of variable importance used the same procedures as base model selection. For nutritional covariates, a new set of candidate models was created by adding K and BFI to the base model as covariates, as both were identified as influential to fecundity in other species (Murua et al. 2003, Tanaka et al. 2017). Disease and location covariates were tested in two model sets that function by testing a model with one additional covariate ("effect model") against the base model, as was described as the information-theoretic methodology replacement to traditional significance testing (Burnham and Anderson 2002, Burnham et al. 2011). Significance is determined by the magnitude and direction of difference between the effect model and the base model. Disease covariates tested were total gross pathology score (HAI), hepatosomatic index (HSI), and mycobacteriosis infection presence/absence as determined by positive acid-fast stain signature (AF). The influence of habitat quality was tested in the same manner as disease, with the base model representing the Choptank River population, and the effect model representing the Severn River population.

In order to better explain the significance of additional covariates on the fit of the model, traditional goodness-of-fit statistics (R^2) were investigated as well as effect size. Partial omega squared (ω^2) effect size estimations were used to quantify each variable's effect on fecundity, following ranking criteria of Field (2013) with 0.01 a small effect, 0.06 a medium effect, and ≥0.14 a large effect (Parveen et al. 2020). All models are additionally checked for covariance using the variance inflation factor (VIF), calculated by (1/1- R_i^2) for each variable in the each of the top-performing

models. Thresholds for collinearity were adapted from accepted thresholds of 1 indicating no collinearity, between 1 and 5 indicating moderate collinearity, and >5 indicating high collinearity, with additional interpretation of other influential factors as described by O'Brien (2007) (Dodge 2008).

3.4 Results

3.4.1 Fecundity Results

In 2018, 109 white perch were sampled from 2 river systems for total estimated fecundity using partially automated gravimetric sampling methods (Table 2.1). Gravimetric fecundity estimates in sampled populations of white perch range from 19723 oocytes per ovary to 280537 oocytes per ovary, with a mean finding of 109145 oocytes per ovary. Severn River fish (n=43) had a mean fecundity of 114578 and Choptank River populations (n=66) had mean fecundity of 117164 (Figure 2.6). When compared to findings from historically and geographically distinct studies, estimates from the Choptank and Severn Rivers fall within range of other reported population fecundity values, specifically 50000-150000 in the Chesapeake, and overall ranges from all studies of 5000 to 300000 eggs.

In addition to 2018 sampling in the Choptank, 116 additional white perch were stereologically sampled for fecundity analysis from 2015, 2016 and 2017. Average fecundity was 38812, 25340, and 65521 for years 2015, 2016 and 2017 respectively. Correlation investigation with the Choptank juvenile index, collected yearly for stock assessment purposes by MDNR, yielded weak positive correlation (Pearson's r = 0.32).

3.4.2 Base Model Selection

Five candidate models, including a null model of only the intercept were used for base model selection, in different combinations of TL, TW and A (Table 3.2). The model with TW and A as covariates was selected as the most parsimonious with an AICw of 0.66. This model was 50% more likely to be the best in the set compared to a model with TL and A, and 92% more likely than a model with TL and A. None of the covariates, when used individually, produced competitive AICw values. Models with only TW and TL also scored similarly low, indicating the importance of A as a covariate. Partial omega squared (ω^2) values showed large of effect of TW (0.30) and no effect (0.00) of age on fecundity (Table 3.8).

3.4.3 Nutrition and Fecundity

The addition of the nutritional covariates condition factor (K) and visceral body fat index (BFI), yielded positive results in model selection procedures. The model with both covariates performed the best in selection procedures, with an AICw of 0.77, translating to a 77% chance of being the best model as compared to the base model (Table 3.4). The two-parameter model was 65% more likely the best selection over a model with only K as an additional covariate and 71% more likely the best selection over a model with BFI as the only additional parameter. Total weight continued to have the largest effect ($\omega^2 = 0.30$), though BFI and K showed moderate effect with ω^2 of 0.06 and 0.03 respectively.

3.4.4 Disease and Fecundity

Disease covariates were investigated in three distinct, two model sets, all of which were evaluated based on information-theoretic methods (Table 3.5). The model containing the gross pathology index score (HAI) as a covariate was 0.7% less likely to be the best fit than the base model, with both the effect model and base model having around a 50% chance of being the best fit. This result was similar to those of the model containing hepatosomatic index values as an additional covariate, which was 50% less likely to be the best model when compared to the base model. The magnitude and direction of these findings indicate lack of significant impact from both HAI and HSI on white perch fecundity. Lack of impact is corroborated by small effect size for HAI ($\omega^2 = 0.01$) and HSI ($\omega^2 = 0.00$).

The model containing mycobacteriosis infection as a covariate had 99% certainty of being the best model in set, with the base model having a near 0% chance of being the best fit (Table 3.5), which by convention indicates a strong influence on model accuracy (Burnham et al. 2011). This is corroborated by visual inspection with regard to the effects of mycobacterial infection on fecundity, as plots show a difference in means for fecundity in infected and non-infected specimens (Figure 3.6). Calculated mean fecundity with mycobacteriosis infection is 71908 as compared to 81057 mean fecundity without signs of infection. Effect size however shows mycobacteriosis to have no impact on model variance ($\omega^2 = 0.00$).

3.4.5 Geographic Comparison

The comparison of geographically discrete populations in the Severn and Choptank sub-estuaries was to determine potential anthropogenic influence on

fecundity, based on watershed usage and contaminant loading. Land use analysis of watersheds indicated Severn River watershed was 42% urban/suburban, with 16% impervious surface coverage, and Choptank River watershed was 11% urban/suburban with 2.8% impervious surface coverage (Matsche et al. in press). Contaminants sampling of non-tidal locations in both watersheds, yielded higher concentrations of water column PAH, organochlorine, and BDE compounds in Severn River samples (Matsche et al. in press). Levels of PAH compounds were 7 to 36 times higher in the Severn River, organochlorines were 2.8 to 7 times higher in the Severn River with the exception of Toxaphene, and BDE compounds were 1.7 to 2.5 times higher in the Severn River (Matsche et al. in press). Health assessment index values between the two populations showed increased total gross pathology values and hepatosomatic index values in Severn River populations (Figure 3.6).

Differences in average white perch fecundity values between the Severn and Choptank Rivers were small in magnitude, with an average fecundity in the Choptank River for 2018 of 117164 and 114578 in the Severn River (Table 3.1). Model selection indicated that the model with Severn River included was 6% more likely the best model as compared to the base model containing only Choptank River samples. The magnitude of ΔAIC_c between the two, however, is only 0.12, indicating insignificant difference between the two models (Table 3.6). Largest effect size continued to be attributed to total weight ($\omega^2 = 0.72$), with location only having a small influence ($\omega^2 = 0.01$).

3.5 Discussion

Superficially, fecundity results from the current study falling within range of historical estimates may indicate no noticeable change in white perch fecundity from the late 1950s. Yet, due to the small home-ranges of white perch populations in the Chesapeake Bay, conclusions can only be drawn about the Severn and Choptank sub-estuaries (Kraus and Secor 2004, McGrath 2009). Due to this putative, compartmentalized nature of white perch populations, any regional estimates would likely need more sampling coverage. Further complicating historical comparisons is the fact that the original source material from 1961 does not provide information on sampling methodology (Mansueti 1961). Even without knowing morphometric characteristics of sampled individuals, sampling for studies in the 1950s was done on the Patuxent River, a different system in the Chesapeake Bay, which does not enable direct comparisons to identify change over time.

While current fecundity estimates are similar in magnitude to historical estimates for the region, the simple comparison of fecundity counts over time only provides limited insight into population fecundity trends. The analysis of Choptank River white perch fecundity data as a 4-year time series allows for a deeper understanding of the drivers of fecundity variation, either between populations or individuals. The creation of a "base" model from which to add additional parameters (i.e. condition factor and disease) for the purposes of variable significance testing serves as a means to substitute information-theoretic methods for traditional null-hypothesis testing while controlling for variance caused by morphometric characteristics. The importance of fish weight to fecundity in particular is well-established in many species and is unsurprisingly important for Chesapeake Bay

populations of white perch as determined by model selection outcomes for the base model candidate set (Cooper et al. 2005, Okoye et al. 2008, Tanaka et al. 2017). Omega-squared effect size estimates confirm this importance, with each model containing total weight registering at least $\omega^2 = 0.30$. Despite its inclusion in the "base" model, age appears to have almost no influence on individual fecundity, contrary to findings in other perch fecundity work (Mansueti 1961, Okoye et al. 2008). This is possibly due to the use of a total length range of 180mm to 240mm in the MDNR health assessment study, for the purpose of controlling the effects of age on disease loading. While this range eliminates the possibility of collecting immature fish for fecundity study, it also truncates the age distribution of collected specimens.

Adding nutritional parameters to the base model yielded apparent significance, in that the model including Fulton's condition factor (K) and observed visceral body fat (BFI), was 23 times more likely than the base model to be the best fit. While this indicates some influence of both K and BFI on model accuracy, ΔAICc scores were only 6.27 for the unparameterized base model as compared to the best performing model. This difference is small by conventions of information-theoretic model selection and points to an interpretation of more limited influence of K and BFI variables on fecundity (Burnham and Anderson 2002). Effect size estimates further confirm the limited effect of nutritional covariates, with both reflecting small to medium effect on model variance.

The influence of disease on fecundity is more difficult to determine than the influence of nutrition, as the pathology of different conditions can influence the quality of oocytes but most do not seem to affect the number of oocytes produced (Blazer 2002, Kavanagh et al. 2004, Blazer et al. 2013). Gross pathology index

scores present a good preliminary analysis, in that the index values do not reflect any specific pathogens but rather the overall pathology burden, which is similar in practice to nutritional condition indicator variables. While MDNR data continues to support higher total gross pathology index scores in degraded areas (Figure 3.6), results show no positive correlation between total HAI scores and lower fecundity as indicated by the outperformance of the model containing HAI as a covariate by the base fecundity model. This finding is possibly due to the methodology of the HAI. Index style sampling presents a more topical approach to determining population health and has limited effectiveness on the individual level (Adams et al. 1993, MDNR unpublished data).

More specific disease covariates including the hepato-somatic index (HSI), and mycobacteriosis infection were selected to augment HAI study, specifically because of their relevance to specific pathogens present in Chesapeake Bay white perch populations. Despite past and present study showing increased average HSI in degraded habitat, model selection and effect size investigation showed no effect of HSI on fecundity (McLaughlin et al. 2018, MDNR unpublished data). Lack of influence of HSI on model performance (Table 3.4) may also indicate no influence on fecundity from recently discovered, chronic coccidiosis in white perch in the Chesapeake Bay. However, on-going MDNR research has shown the recently discovered coccidian parasite *Goussia bayae* increases tumor prevalence but does not affect hepato-somatic index (HSI) values in white perch. This finding may indicate that HSI values cannot be used as a proxy for impacts of coccidiosis (Matsche et al. 2019b, MDNR unpublished research). Explanation for this consideration may lie in the limited role of the liver in oocyte production. The liver produces vitellogenin, an

important protein for oocyte development, but this production does not affect the number of eggs, only the quality. Vitellogenin sampling, or lipid content of eggs, is a logical next step to therefore determine if, despite having no impact on fecundity, coccidians in the biliary fluids are impacting liver health, and thus oocyte viability.

As discussed, mycobacterial infection in the teleost species of the Chesapeake Bay is an important covariate, due to its high prevalence compared to other geographic locations (Kane et al. 2007, Jacobs et al. 2009, Matsche et al. 2013). The magnitude of difference between the base model and the model with the additional covariate of mycobacteriosis presence/absence indicates a significant impact of the disease on fecundity (Table 3.4, Figure 3.6). Effect size findings however contradict this level of significance with no effect found on model variance as a result of mycobacteriosis infection, leaving the impact of mycobacteriosis on white perch fecundity inconclusive (Table 3.8). Even in the closely related striped bass, research has also suggested a link between mycobacteriosis infection and failing reproductive health is difficult to find, despite high disease prevalence (>50%) in the Chesapeake population (Matsche et al. 2013, Gervasi et al. 2019, MDNR unpublished data). This lack of correlation may possibly be because the disease is changing the survival of individuals, leading to their removal from the population before reaching maturity (Gervasi et al. 2019). In comparison, mycobacteriosis in Chesapeake Bay white perch presents with much milder symptoms than in striped bass, and lower overall prevalence (<30%) (Jacobs et al. 2009, MDNR unpublished data). If this is an indication of less virulence, it is possible that mycobacteriosis is causing less mortality in white perch, but instead is causing reproductive stress and lower fecundity. While mycobacteriosis infections have been widely studied in fish,

reproductive effects of the disease are seldom noted, making inconclusive findings unsurprising. Infections have been documented as a nuisance in aquaculture for many years but due to the nature of captive fish breeding and the lack of effective non-lethal treatments, infected fish are typically culled, eliminating the possibility to study reproductive effects (Gaunthier and Rhodes 2009, Jacobs et al. 2009). Further study is needed, specifically in the highly infected Chesapeake Bay striped bass populations, to determine the magnitude of potential fecundity impacts.

Given the potential for at least certain pathology to affect fecundity, anthropogenic influences that lead to greater stress and disease in fish could theoretically lead to lower population fecundity. Environmental degradation, in the form of sediment contamination and hypoxic conditions, has been shown to impact white perch fish condition in the Chesapeake Bay, with lower nutritional index values and higher gross pathology values in degraded locations, all of which have the potential to effect fecundity. Previously published impacts of habitat degradation on white perch included lower neutrophil and leukocyte counts, higher hepatic tumor prevalence, higher internal parasite burden, and higher densities of macrophage aggregates in splenic tissue (Morgan et al. 1973, King et al. 2004, McLaughlin et al. 2018).

While comparisons of Chesapeake Bay-wide data between past and present studies are not definitive, the Severn and Choptank Rivers are documented to have different levels of habitat quality, therefore enabling direct comparisons as to the effects of habitat quality on reproductive potential in white perch (Uphoff et al. 2011, Matsche et al. in press). Lower fecundity was hypothesized for Severn River white perch populations due to documented local reproductive failures in yellow perch, and

higher levels of environmental degradation (Uphoff et al. 2011, Blazer et al. 2013). While evidence exists correlating elevated industrial and residential land-use in the Chesapeake Bay watershed to higher levels of gross pathology and higher tissue contaminant levels in white perch, this study seems to refute any noticeable impacts on population fecundity (King et al. 2004, McLaughlin et al. 2018). Differences between models with and without location as a covariate were small enough to be deemed insignificant by convention, which corroborates simple visual inspection of the population fecundity values in the Severn and Choptank Rivers (Burnham and Anderson 2002). Previous findings on the reproductive effects of contamination were limited to populations directly exposed in controlled settings or near point-source discharges, which, given the random site selection methods used in this study, would explain lack of definitive results (Monosson et al. 1994, Kavanagh et al. 2004). Adding more subtle indicators of reproductive health such as vitellogenin levels to future studies could provide more insight into effects of environment on white perch reproductive capacity.

It is also possible that the abundance of white perch is serving to dampen the impacts of environmental degradation as was observed in the Hudson River estuary, where despite locally high levels of PCB contamination, the effects on population-wide reproduction were dampened by abundance of white perch (Barnthouse et al. 2009). Findings of Barnthouse et al. (2009) indicate that despite certain sub-populations of white perch in the Hudson River living in highly contaminated areas, the population was large enough to still support high recruitment, even if individuals in contaminated areas possibly have lower fecundity. If abundance of white perch in the Chesapeake is responsible for similar phenomenon, more specific site selection in

documented areas of heavy contamination might yield different results, but this study shows that reductions in fecundity of small sub-populations might not have any impact.

Despite lack of apparent negative impact on fecundity from degraded habitat, from a management standpoint, the addition of reproductive data to stock assessments may prove advantageous for assessing the health of Chesapeake Bay fish populations. The Bay faces heavy anthropogenic influence and possible impacts from climate change, both of which may affect fish stocks adversely through increases in stress and disease. While abundant populations can absorb adverse effects of disease on fecundity, should disease prevalence increase, or fitness decline, reproductive output of white perch populations may decline as a result. This study has demonstrated the utility of investigating drivers of fecundity variation through AIC modeling techniques, that when translated to other stocks in the Chesapeake region which are experiencing reproductive failures, will enable more precise management of local stocks for the challenges of the future.

3.6 Tables and Figures

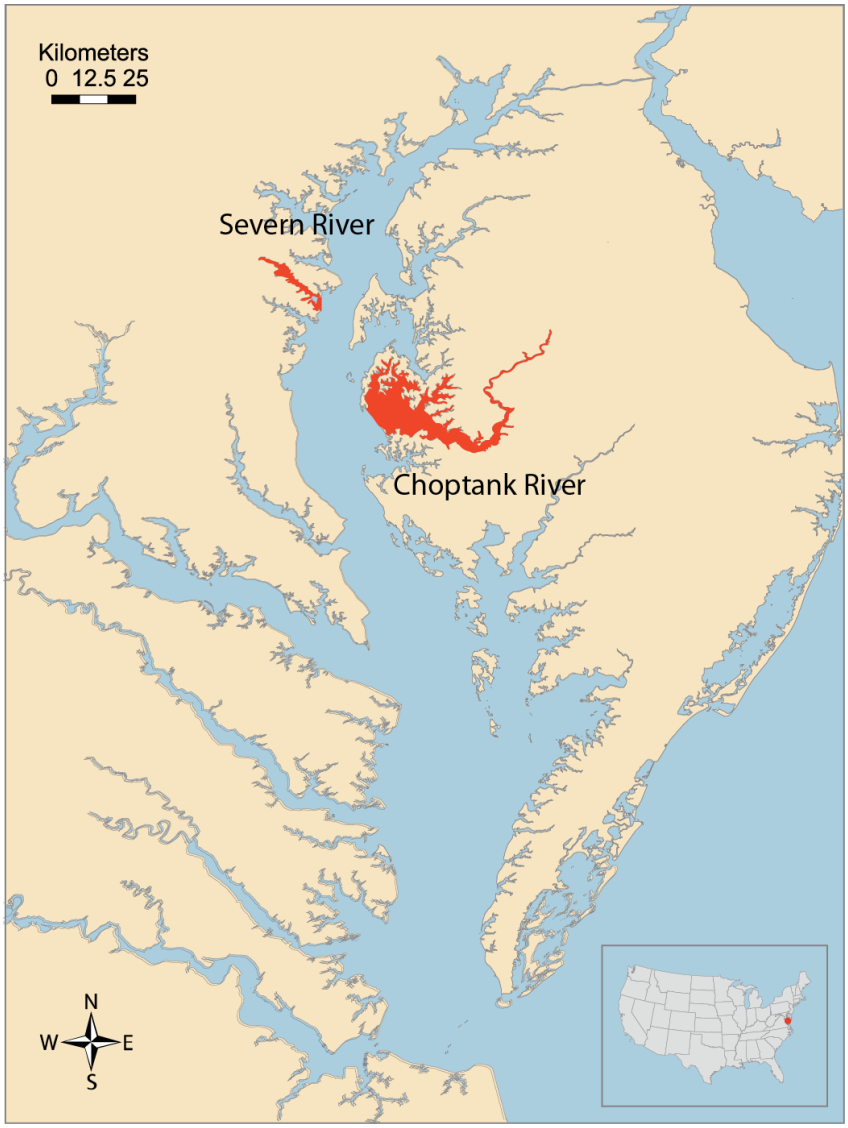

Figure 3.1 Sampling locations for white perch in Chesapeake Bay. Both highlighted rivers shown were sampled in 2018, but only Choptank River locations were sampled 2015-2017. Map image: T. Saxby, K. Boicourt, Integration and Application Network, University of Maryland Center for Environmental Science (ian.umces.edu/imagelibrary/).

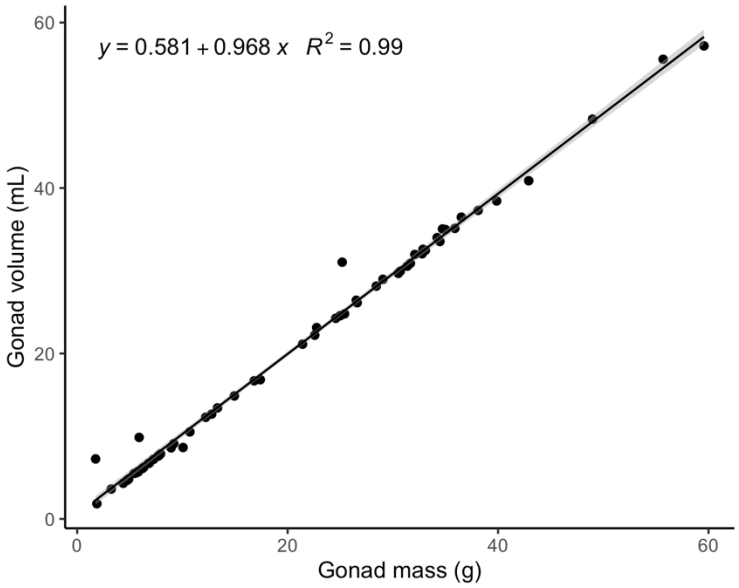

Figure 3.2 Linear model results of the comparison between gonad mass and gonad volume of pre-spawn white perch. Gonad volume was obtained using the wet weight method (Scherle 1970). $N = 61$ fish, collected in spring of 2020 with gonad mass ranging from <1 g to 60 g.

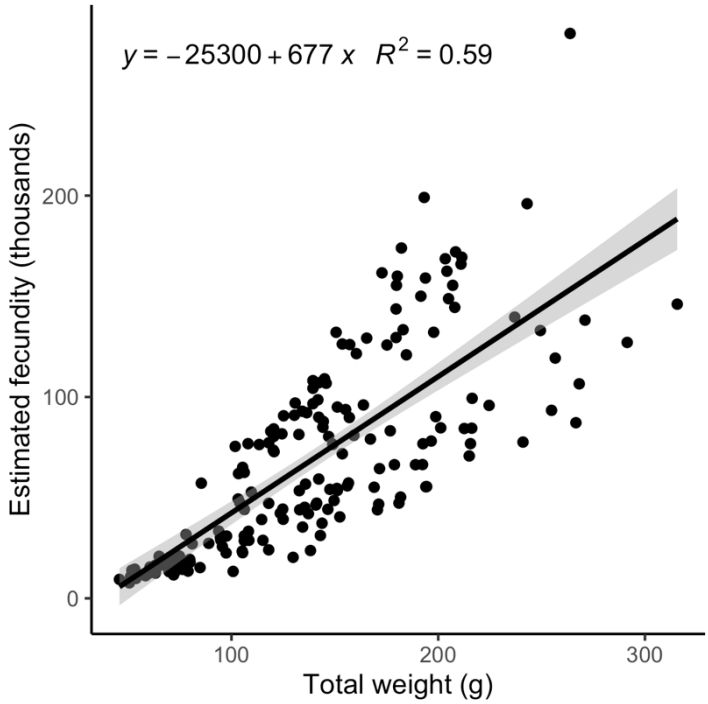

Figure 3.3 Relationship of white perch fecundity to total fish weight for all sampling locations. Plot shows positive correlation identified in model selection.

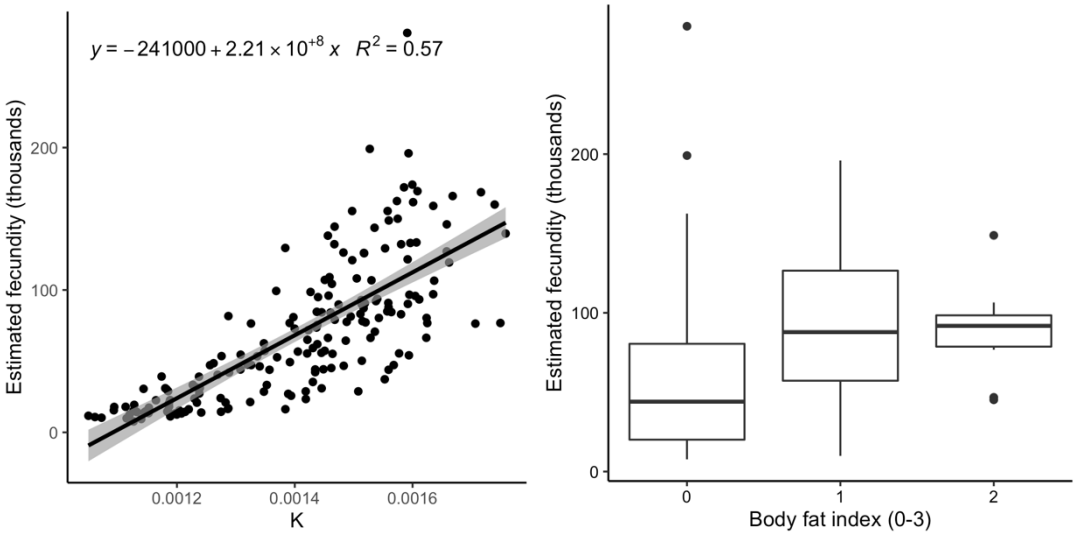

Figure 3.4 Influence of nutritional indicator variables on white perch fecundity. Values of Fulton's condition factor (K) and body fat index, which is the presence and amount of visceral body fat, indicate foraging success and food availability. High values are hypothesized to indicate increased energy allocation to egg production.

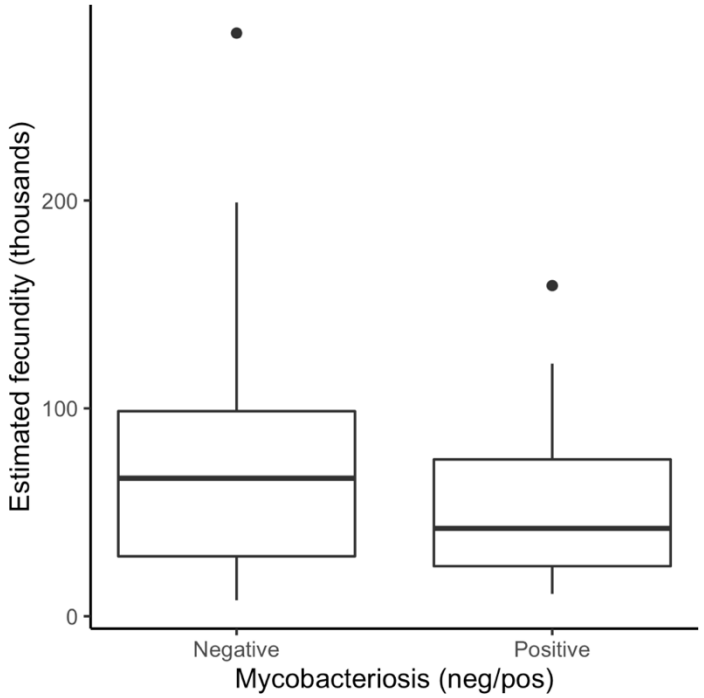

Figure 3.5 Influence of mycobacteriosis infection on white perch fecundity in the Chesapeake Bay. Mycobacteriosis survey involves presence/absence (as shown by negative and positive for infection) but not severity of infection.

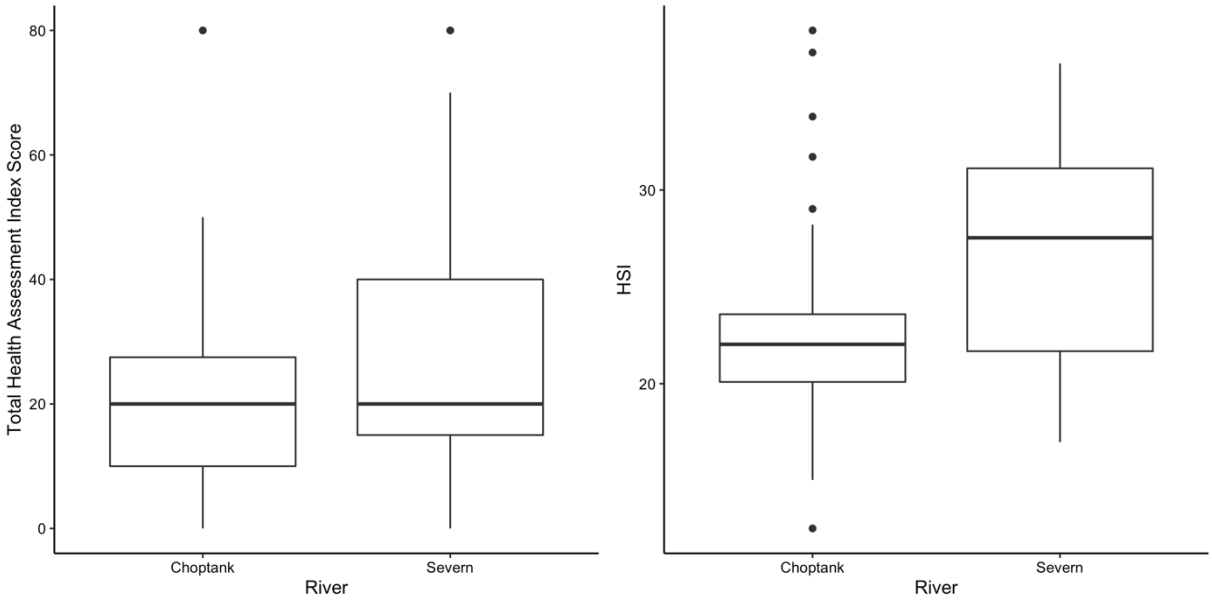

Figure 3.6 Differences in white perch pathology between the Severn and Choptank Rivers. MDNR studies on the Tred Avon River have shown increased Total Health Assessment Index Scores and increased liver pathology, shown by increased hepato-somatic index (HSI) values in degraded habitats. Higher values of both indices on the Severn River support conclusions of increased degradation.

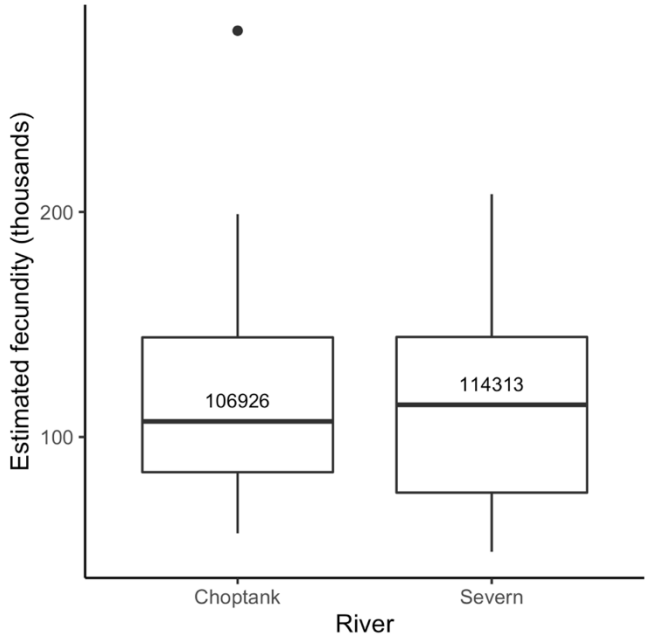

Figure 3.7 Results of 2018 riverine comparison of white perch fecundity, in number of eggs per fish. Value listed is median fecundity of white perch for each river.

Table 3.1 White perch fecundity results by year for each river used in the analysis.

	NUMBER OF FISH	AVERAGE FECUNDITY	MIN	MAX
CHOPTANK RIVER	182	**70141.09**	**7691**	**280537**
2015	51	38811.63	9399	138157
2016	30	25340.43	7691	84345
2017	35	65520.77	28592	146092
2018	66	117164.3	57184	280537
SEVERN RIVER	43	**114578.1**	**48968**	**207941**
2018	43	114578.1	48968	207941

Table 3.2 Model selection results to determine the influence of morphometric and life history covariates on white perch fecundity (F), in order to select a base model for later addition of disease and nutritional covariates. Covariates include total weight (TW), total length (TL), and age (A). Reported parameters include Akaike's Information Criterion, adjusted for small sample size (AICc), ranked from lowest to highest (lowest is best), as well as ΔAICc listed as the difference between the highest ranking model and the current model, and AICw, relative weight of the difference. Null model is a model with no additional covariates. Best fitting model based on these criteria includes covariates of TW and A.

Model	*AICc*	*ΔAICc*	*AICw*	*Likelihood*	R^2
F~TW+A	2415.72198	0	0.66206051	1	0.32
F~TL+TW+A	2417.40331	1.68133642	0.28562756	0.43142215	0.32
F~TL+A	2420.79824	5.07626527	0.05231192	0.07901381	0.28
F~A	2452.40332	36.6813401	7.17E-09	1.08E-08	<0.01
F~TL+TW	4284.19115	1868.46918	0	0	0.61
F~TW	4294.70766	1878.98568	0	0	0.59
F~TL	4335.97459	1920.25262	0	0	0.48
Null	4452.87482	2037.15284	0	0	-

Table 3.3 Health Assessment Index (HAI) metrics used by MDNR to determine impacts of habitat condition on fish populations. Except where indicated, lesions are scored on overall subjective severity from no lesions or abnormalities (0), mild (10), moderate (20), and severe (30). Total HAI score is calculated by totaling the scores from all categories. Multiple conditions in one organ or group are summed. Used with permission from MDNR standard operating procedures.

Organ	Lesion	Criteria	Score
External			
Eyes	Exophthalmia	Extent of swelling/protrusion	0, 10, 20, 30
	Cataract	Opacity on eye(s)	0, 10, 20, 30
	Hemorrhage	Bleeding in eye(s)	0, 10, 20, 30

	Blind	Damage or deformation to eye(s)	30/eye
	Missing	One or both eyes	30/eye
	Other	Other condition not covered above	0, 10, 20, 30
Skin	Ulcer	Necrotic erosions of skin	0, 10, 20, 30
	PF	None (0), 1-10 (10), 11-50 (20), >50 (30)	0, 10, 20, 30
	Scale Loss	Amount of loss (not scored for ulcers)	0, 10, 20, 30
	Redness	Focal, multifocal or diffuse	0, 10, 20, 30
	Tumor	Any mass or swelling	0, 10, 20, 30
	Other	Other condition not covered above	0, 10, 20, 30
Fins	Redness	Focal, multifocal or diffuse	0, 10, 20, 30
	Erosion	Necrosis, often with depigmentation	0, 10, 20, 30
	Damaged	Bent, broken, or deformed	0, 10, 20, 30
	Other	Other condition not covered above	0, 10, 20, 30
Gills	Erosion	Necrotic filaments, frayed appearance	0, 10, 20, 30
	Pale	Loss of red color	0, 10, 20, 30
	Clubbed	Rounded, swollen filament tips	0, 10, 20, 30
	Other	Other condition not covered above	0, 10, 20, 30
Internal			
Heart	Flaccid	Soft, watery consistency	30
	Nodular	One or more nodules present	0, 10, 20, 30
	Other	Other condition not covered above	0, 10, 20, 30
Liver	Discolor	Focal or multifocal color changes	0, 10, 20, 30
	Fatty	Cream color, rounded margins	0, 10, 20, 30
	Nodular	One or more nodules present	0, 10, 20, 30
	Adhesions	Fibrous connections with other tissues	0, 10, 20, 30
	Other	Other condition not covered above	0, 10, 20, 30
Spleen	Granular	Fine grained texture on surface	0, 10, 20, 30
	Nodular	One or more nodules present	0, 10, 20, 30
	Abscess	One or more fluid-filled pockets	0, 10, 20, 30
	Adhesions	Fibrous connections with other tissues	0, 10, 20, 30
	Other	Other condition not covered above	0, 10, 20, 30
Intestine	Redness	Focal, multifocal or diffuse	0, 10, 20, 30
	Swollen	Enlarged or swollen area(s)	0, 10, 20, 30
	Adhesions	Fibrous connections with other tissues	0, 10, 20, 30
	Other	Other condition not covered above	0, 10, 20, 30
Kidney	Swollen	Enlarged or swollen area(s)	0, 10, 20, 30
	Mottled	Focal or multifocal color changes	0, 10, 20, 30
	Nodular	One or more nodules present	0, 10, 20, 30
	Uroliths	Calcium deposits, "crunchy"	0, 10, 20, 30
	Other	Other condition not covered above	0, 10, 20, 30
Other			
Parasites	External	None (0), Few (10), More (20), Many (30)	0, 10, 20, 30
	Internal	None (0), Few (10), More (20), Many (30)	0, 10, 20, 30

Table 3.4 Results from model selection for models with additional nutritional covariates of Fulton's Condition Factor (K) and observed visceral body fat index values (BFI). The model containing both K and BFI was most parsimonious but models with other combinations of covariates as well as the base model (TW+A) were within a plausible range, indicating only weak influence of nutritional covariates (<7 ΔAICc).

Model	*AICc*	*ΔAICc*	*AICw*	*Likelihood*	R^2
F~TW+A+K+BFI	2409.44894	0	0.77865884	1	0.39
F~TW+A+BFI	2413.14123	3.6922911	0.12290694	0.1578444	0.35
F~TW+A+K	2414.42722	4.97828109	0.06461409	0.08298125	0.34
F~TW+A	2415.72198	6.27303341	0.03382013	0.04343383	0.32
Null	4452.87482	2043.42587	0	0	-

Table 3.5 Combined table of disease candidate model sets, with the first set containing a covariate of total health assessment index score (Total HAI), second containing hepatosomatic index (HSI), and third containing mycobacteriosis presence/absence determined by acid-fast staining (AF). Total HAI and HSI show no influence over fecundity, determined by lower ΔAICc scores than the base model (TW+A). Mycobacteriosis as a covariate exerts a strong influence on model performance with the base model showing >14 ΔAICc when compared.

Model	*AICc*	*ΔAICc*	*AICw*	*Likelihood*	R^2
F~TW+A	2415.72198	0	0.5018705	1	0.32
F~TW+A+HAI	2415.73694	0.01496405	0.4981295	0.9925459	0.34
Null	4452.87482	2037.15284	0	0	-
F~TW+A	2415.72198	0	0.67860917	1	0.32
F~TW+A+HSI	2417.21675	1.49477491	0.32139083	0.47360224	0.32
Null	4452.87482	2037.15284	0	0	-
F~TW+A+AF	2319.54437	0	1	1	0.34
F~TW+A	2415.72198	96.1776019	1.30E-21	1.30E-21	0.32
Null	4452.87482	2133.33044	0	0	-

Table 3.6 Addition to base model (Total weight+age) of Severn River samples as a covariate ("River"), to determine if populations in a comparatively degraded habitat are affected by increases in total disease pathology and stress. Selection procedures show weak evidence of difference (<1 ΔAICc).

Model	*AICc*	*ΔAICc*	*AICw*	*Likelihood*
F~TW+A	2492.4643	0.12531957	0.48434018	0.93926297
F~TW+A+River	2492.33898	0	0.51565982	1

Table 3.7 Variance inflation factor (VIF) results for each model used in analysis, by variable. Variables include total weight (TW), age (A), condition factor (K), observed body fat index (BFI), total health assessment index score (HAI), hepatosomatic index (HSI), mycobacteriosis presence (AF) and location (L). VIF factors are below conservative thresholds of 2.5, indicating no collinearity.

Model	***Independent variables***					
F~TW+A	**TW**		**A**			
VIF		1.03		1.03	-	-
F~TW+A+K+BFI	**TW**		**A**		**K**	**BFI**
VIF		1.51		1.07	1.53	1.09
F~TW+A+HAI	**TW**		**A**		**HAI**	
VIF		1.03		1.04	1.01	-
F~TW+A+HSI	**TW**		**A**		**HSI**	
VIF		1.16		1.04	1.13	-
F~TW+A+AF	**TW**		**A**		**AF**	
VIF		1.04		1.03	1	-
F~TW+A+L	**TW**		**A**		**L**	
VIF		1.13		1.12	1.02	-

Table 3.8 Omega squared (ω^2) effect size results for each model used in analysis, by variable. Variables include total weight (TW), age (A), condition factor (K), observed body fat index (BFI), total health assessment index score (HAI), hepatosomatic index (HSI), mycobacteriosis presence (AF) and location (L). Effect ranked as per Field (2013) with 0.01 = small, 0.06 = medium, ≥0.14 = large.

Model	***Independent Variables***							
F~TW+A	**TW**		**A**					
Effect size		0.3		0		-		-
F~TW+A+K+BFI	**TW**		**A**		**K**		**BFI**	
Effect size		0.32		0		0.03		0.06
F~TW+A+HAI	**TW**		**A**		**HAI**			
Effect size		0.3		0		0.01		-
F~TW+A+HSI	**TW**		**A**		**HSI**			
Effect size		0.3		0		0		-
F~TW+A+AF	**TW**		**A**		**AF**			
Effect size		0.31		0.01		0		-
F~TW+A+L	**TW**		**A**		**L**			
Effect size		0.72		0		0.01		-

Appendix I: Details on stereological pilot studies

A.1 Introduction

This document contains supporting information pertaining to pilot studies performed with stereological fecundity sampling methods of white perch *Morone americana*. Pilot studies were required to determine efficacy of using the method on white perch, as well as diagnosing potential problems with the counting methodology. Error rates between counted fields were determined based on standardized stereological principles (West 2012). It was further necessary to determine how many fields, or grid positions per slide, would provide an accurate sample with error rates below accepted thresholds of 10%, as certain archival samples had smaller amounts of sectioned tissue (West 2012). Methods testing used a standard square grid as opposed to Weibel style counting grids used in prior studies as software only supported the former. Before continuing with fecundity sampling it was imperative to determine if grid style played a significant role in counting accuracy.

A.2 Methods

Pilot studies were performed on 10 fish from the 2018 sampling year, in order to facilitate comparisons with gravimetric data. Preliminary trials were done on one fish at 4x, 10x and 25x with grid sizes of 3000 μm^2, 1000 μm^2, and 500 μm^2, respectively to determine an effective grid size that would maximize efficiency while minimizing error rates between different fields counted from the same sample. Grid sizes were standardized as squares of different sizes during the selection process to enable simpler computation of fecundity as per the formula (Emerson et al. 1990). Following grid selection, trials were done with five samples to determine how many

fields were necessary to obtain a viable fecundity estimate. Samples used needed to support 20 unique frames in which to perform counts without overlap. Error rates were calculated separately for volume and abundance counts, using the following formulas:

$$S^2 = 0.0724 \times (\frac{b}{\sqrt{a}}) \times \sqrt{n} \times \sum P \quad \text{(Equation A.1)}$$

$$Var_{SRS} = \frac{3 \times [A - S^2] - 4 \times B + C}{12} \quad \text{(Equation A.2)}$$

$$Var_{TOTAL} = Var_{SRS} + S^2 \quad \text{(Equation A.3)}$$

$$OCE(\sum P) = \frac{\sqrt{Var_{TOTAL}}}{\sum P} \quad \text{(Equation A.4)}$$

where P is partial area of oocytes in a given grid, n is the number grid fields counted, In equation A.1, the $(\frac{b}{\sqrt{a}})$ term is a shape factor which is the ratio of perimeter divided by the root of the area (West 2012). In Equation A.2, A, B, and C terms relate to sums of partial area values, where A=$\sum(P_i \times P_i)$, B= $\sum(P_i \times P_{i+1})$, and C=$\sum(P_i \times P_{i+2})$, meaning for the whole specimen, each data point (P_i) is either multiplied by itself, multiplied by the next value, or the value twice removed (Table A.1). In order to calculate the observed coefficient of error (OCE, Equation A.4), variance must first be computed for variability between within individual sections (S^2, Equation A.1) and variability between sections (Var_{SRS}, Equation A.2), and added for a total variance (Var_{TOTAL}, Equation A.3). The same procedure is performed separately for the number of objects, N, where the above procedure is for the partial area of objects, P.

During trials, error rates were calculated automatically using pre-formatted spreadsheets in Microsoft Excel in order to consistently monitor error to determine

when error rates were below accepted thresholds. Once error rates were within threshold limits, counts continued to 20 fields. Coefficients of variation (CV) estimates were calculated for each sample in RStudio, using random number generation to randomize fecundity estimates obtained after each subsequent frame. CV estimates were plotted to examine how many frames are necessary for an accurate estimate (Figure A.1). After minimum number of fields was determined, repeatability of estimates was investigated by counting one of the 5 samples selected randomly 5 times.

A.3 Results

Preliminary counts determined that the best compromise between magnification and grid size was the use of 4x optics with a grid size of 3000 μm^2. No observable difference between Weibel grid counts and standard counts was found, so the standard 10 × 10 grid was used for the study. Investigation into CV estimates yielded noticeable variation up to 10 counted sections, with a general leveling of variation after, indicating that 10 sections per fish could be considered a minimum level of counts required (Figure A.1).

A.4 Tables and Figures

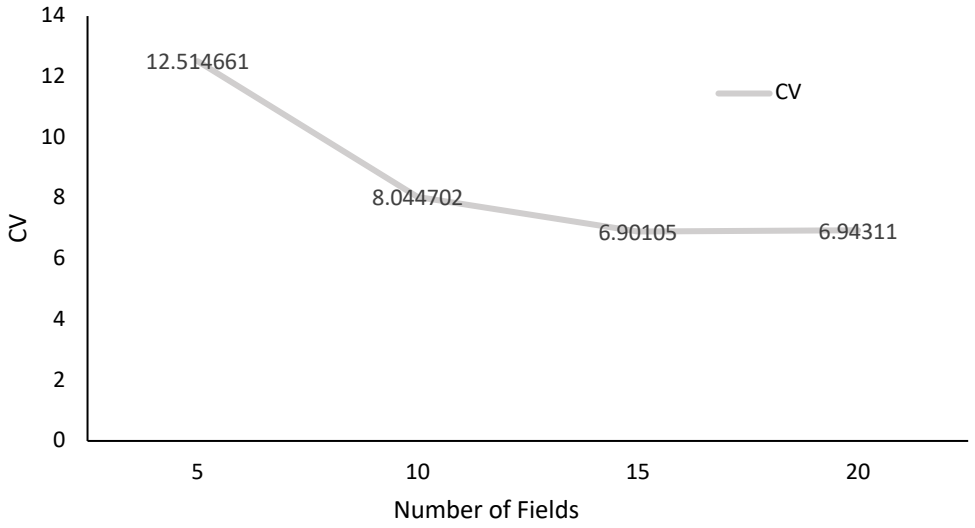

Figure A.1 CV calculations to determine number of counting fields necessary for accurate fecundity estimations. CV estimates were averaged across 5 pilot study specimens, with fecundity estimates randomized using random number generation pairing.

Table A.1 Example of pilot study fecundity data, obtained stereologically, with observed coefficient of error (OCE) calculations. Separate OCE percentages were needed for both area calculations and number counts. The goal of pilot studies was to keep error rates below 10% by adjusting number of grid fields counted per specimen.

Section	N1	N1*N1	N1*N1+1	N1*N1+2	P1	Totalarea	P1*P1	P1*P1+1	P1*P1+2
1	37	1369	1110	1295	56	86	3136	3360	3024
2	30	900	1050	1230	60	91	3600	3240	3840
3	35	1225	1435	1155	54	79	2916	3456	2970
4	41	1681	1353	1353	64	92	4096	3520	4160
5	33	1089	1089	1254	55	84	3025	3575	3795
6	33	1089	1254	1320	65	90	4225	4485	4160
7	38	1444	1520	1444	69	95	4761	4416	4278
8	40	1600	1520	1080	64	96	4096	3968	3456
9	38	1444	1026	1330	62	91	3844	3348	3658
10	27	729	945	918	54	78	2916	3186	3024
11	35	1225	1190	875	59	93	3481	3304	2655
12	34	1156	850	1088	56	90	3136	2520	3360
13	25	625	800	625	45	75	2025	2700	1800
14	32	1024	800	0	60	89	3600	2400	0
15	25	625	0	0	40	78	1600	0	0
	N	A	B	C		P	A	B	C
	503	17225	15942	14967		863	50457	47478	44180
	S2	VAR	VAR total	**OCE**		S2	VAR	VAR total	**OCE**
	503	113.75	616.75	0.049373		31.21732	462.1123	493.3297	0.025737

Appendix II: Code for automation of gravimetric data analysis

A.1 Introduction

This supplemental document contains code written to automate repetitive procedures in both gravimetric and stereological fecundity methods. Macros are for use in ImageJ software, whereas R code is for use in RStudio.

A.2 Methods

A.2.1 Automated particle counting from images

Gravimetric fecundity was automated by macro programming in ImageJ. Macros can be either written by hand or recorded automatically while users go through the desired process in the software interface. Macros are run in ImageJ by selecting Plugins>Macros>Run…,which opens a file browser to locate the macro file. For this particular macro, the first image in the working directory must be open for the macro to successfully run. Images must be edited before running this macro, with the watershed procedure to separate contiguous particles (Figure 2.2). Limited manual editing may be required to remove debris, air bubbles, or glare reflections, though careful photography can eliminate many of the aforementioned issues. Once open the macro will run, with one prompt for the user to check results for each specimen before moving to the next file.

```
//Macro for calculation of gravimetric fecundity

run("Set Scale...", "distance=33.2005 known=1 unit=mm global");

//dir1 = source directory of photos
dir1 = getDirectory("Choose Source Directory");

//dir2 = directory for results
dir2 = getDirectory("Choose Source Directory");
  list = getFileList(dir1);
  for (i=0; i<list.length; i++) {
     open(dir1+list[i]);
```

```
name = getTitle;
run("Make Binary");
run("Analyze Particles...", "size=0.10-Infinity circularity=0.10-1.00 show=Outlines display exclude
clear include summarize");
waitForUser("Check results to check analysis");
saveAs("Results", dir2+name+".csv");
```

The second script below is an R script, designed to identify oocyte clumps that were not eliminated by the watershed procedure during the image editing process. Particles that were larger than the 95th quartile value of each size distribution were deemed groups of oocytes and divided by the mean of the size distribution to yield the number of component particles present in each group. This number was added to the total count to adjust the count results. Accuracy of this procedure was verified by ocular counting of five random samples, which showed differences in counts to be minimal (>5%).

```
#Gravimetric fecundity correction
setwd("path of working directory")

input_files<-list.files("path of working directory",
  pattern=".csv", full.names=FALSE)

#for loop that creates one combined output file for all input files

datalist<-list()

for(i in input_files){
  data<-read.csv(i)
  oocyte<-subset(data, data$Feret>=0.2)
  mean<-mean(oocyte$Area)
  quantile<-quantile(oocyte$Area, 0.95)
  lrg<-subset(oocyte, Area>quantile)
  lrgcorrect<-(lrg$Area/mean)
  sumcorrect<-sum(lrgcorrect)
  initcount<-length(oocyte$Area)
  fincount<-sumcorrect+initcount
  fincount<-round(fincount)
  meandiam<-mean(oocyte$Feret)
  results<-data.frame(Meanferet=meandiam, Initialcount=initcount,Finalcount=fincount)
  datalist[[i]]<-results
}

fulldata<-do.call(rbind, datalist)
write.csv(fulldata, file="name of output file")
```

A.2.2 Automated coefficient calculation, stereological method

Coefficients for each specimen were calculated separately as opposed to using an average value for both. Further study into white perch fecundity and oocyte distribution might yield insignificant difference between specimens, enabling the use of average values. Running data through this process will enable evaluation of variation between individual specimens and calculation of average coefficient values, which could prove useful in pilot studies of stereological fecundity methods for other novel species. As with gravimetric macros described above, limited manual editing is required to ensure particles are adequately separated. Watershed procedures were not as effective for pictures taken at 4x and therefore separation of particles was done manually. This was done before the first prompt ("Adjust threshold and click 'OK'") and verified by the observer before accepting the results. Any particles that were of abnormal shape due to debris or errors in thresholding the image, were noted and manually deleted from results spreadsheet.

```
//Macro for calculation of shape factor and size distribution coefficients for fecundity analysis

run("Set Scale...", "distance=580 known=1 unit=mm global");

//dir1 = source directory of photos
dir1 = getDirectory("Choose Source Directory");

//dir2 = directory for results
dir2 = getDirectory("Choose Source Directory");
  list = getFileList(dir1);
  for (i=0; i<list.length; i++) {
     open(dir1+list[i]);
name = getTitle;
run("8-bit");
setAutoThreshold("Default");
run("Threshold...");
waitForUser("Adjust threshold, then click 'OK' ");
setOption("BlackBackground", false);
run("Convert to Mask");
run("Analyze Particles...", "size=0.05-Infinity circularity=0.10-1.00 show=Outlines display exclude
clear include summarize");
waitForUser("Check outlines to check editing");
saveAs("Results", dir2+name+".csv");
close();close();}
```

The following script is for calculation of coefficients for each specimen from raw data created by above ImageJ macro. Each file of raw particle data was combined to calculate coefficients used for stereological fecundity calculations.

```
setwd("name of working directory")

input_files<-list.files("name of working directory",
  pattern=".csv", full.names=FALSE)

datalist<-list()

for(i in input_files){
  data<-read.csv(i)
  oocyte<-subset(data, data$Feret>0.2 & data$Feret<0.9)
  meandiam<-(mean(oocyte$Feret))
  diam3<-mean(oocyte$Feret^3)
  shape<-mean(oocyte$Feret/oocyte$MinFeret)
  K<-((diam3^(1/3))/meandiam)^(3/2)
  results<-data.frame(K=K,Shape=shape)
  datalist[[i]]<-results
}

fulldata<-do.call(rbind, datalist)
write.csv(fulldata, file="name of output file")
```

Works Cited

Adams S.M., Brown A., Goede R. (1993) A quantitative health assessment index for rapid evaluation of fish condition in the field. Transactions of the American Fisheries Society 122:63-73

Adams S.M., Ham K.D., Greeley M.S., LeHew R.F., Hinton D.E., Saylor C.F. (1996). Downstream gradients in bioindicator responses: point source contaminant effects on fish health. Canadian Journal of Aquatic Science 53: 2177-2187

Barnthouse L.W., Glaser D., DeSantis L. (2009) Polychlorinated biphenyls and Hudson River white perch: Implications for population-level ecological risk assessment and risk management. Integrated Environmental Assessment and Management 5(3): 435-444

Barton B.A., Morgan J.D., Vijayan M.M. (2002) Physiological and condition-related indicators of environmental stress in fish. In: Adams, SM (ed). Biological indicators of aquatic ecosystem stress. American Fisheries Society, Bethesda, Maryland. p 111-148.

Blazer V.S. (2002) Histopathological assessment of gonadal tissue in wild fishes. Fish Parasitology and Biochemistry 26: 85-101

Blazer V.S., Iwanowicz L.R., Iwanowicz D. D., Smith D. R., Young J. A., Hedrick J.D., Foster S.W., Reeser S.J. (2007) Intersex (Testicular Oocytes) in Smallmouth Bass from the Potomac River and Selected Nearby Drainages, Journal of Aquatic Animal Health, 19(4): 242-253

Blazer V.S., Iwanowicz D.D., Walsh H.L., Sperry A.J., Iwanowicz L.R., Alvarez D.A., Brightbill R.A., Smith G., Foreman W.T., Manning R. (2014)

Reproductive health indicators of fishes from Pennsylvania watersheds: association with chemicals of emerging concern. Environmental Monitoring and Assessment 186: 6471-6491

Blazer V.S., Pinkney A.E., Jenkins J.A., Iwanowicz L.R., Minkkinen S., Draugelis-Dale R.O., Uphoff J.H. (2013) Reproductive health of yellow perch *Perca flavescens* in selected tributaries of the Chesapeake Bay. Science of the Total Environment 447: 198-209

Bland J.M., Altman D.G. (1986). Statistical method for assessing agreement between two methods of clinical measurement. The Lancet 327:307-310

Boesch D.F., Brinsfield R.B., Magnien R.E. (2000) Chesapeake Bay Eutrophication. Journal of Environmental Quality 30: 303-320

Boynton W.R., Garber J.H., Summers R., Kemp W.M. (1995) Inputs, Transformations, and Transport of Nitrogen and Phosphorous in Chesapeake Bay and Selected Tributaries. Estuaries and Coasts. 18: 285-314

Boyd J.B. (2011) Maturation, fecundity, and spawning frequency of the Albemarle/Roanoke striped bass stock. PhD dissertation, East Carolina University, Greenville, NC.

Brown S.C. (2017). Personal communication to the author. Email

Bur M.T. (1986). Maturity and fecundity of the white perch, *Morone americana*, in western Lake Erie. Ohio Journal of Science 86(5): 205-207.

Burnham K.P., Anderson D.P. (2002). Model selection and multimodel inference: a practical information-theoretic approach, 2nd edition. Springer-Verlag, New York, New York.

Burnham K.P., Anderson D.P., Huyvaert K.P. (2011). AIC model selection and multimodel inference in behavioral ecology: some background, observations, and comparisons. Behavioral Ecology and Sociobiology 65: 23-35.

Busch W.M., Davies D.H., Nepszy S.J. (1977). Establishment of white perch (*Morone americana*) in Lake Erie. Journal of the Fisheries Research Board of Canada. 34:1039-1041

Cooper D.W., Pearson K.E., Gunderson D.R. (2005). Fecundity of shortspine thornyhead (*Sebastolobus alascanus*) and longspine thornyhead (*S. altivelis*) (Scorpaenidae) from the northeastern Pacific Ocean, determined by stereological and gravimetric techniques. Fisheries Bulletin 103:15-22

Costa E.F.S., Dias J.F., Murua H. (2016) Fecundity of fishes inhabiting coastal and estuarine environments in the southwest Atlantic Ocean. Marine Biology Research, 12(3): 304-315.

Dauer D.M., Weisburg S.B., Ranasinghe J.A. (2000) Relationships between benthic community condition, water quality, sediment quality, nutrient loads, and land use patterns in the Chesapeake Bay. Estuaries and Coasts 23(1): 80-96

Davies A.J., Ball S.J. (1993) The Biology of Fish Coccidia. Advances in Parasitology 32:294-358

Dodge, Y. (2008). The Concise Encyclopedia of Statistics. Springer Science & Business Media.

Emerson L.S., Greer Walker M., Witthames P.R. (1990). A stereological method for estimating fish fecundity. Journal of Fish Biology 36: 721-730

Field A. (2013). Discovering statistics using IBM SPSS Statistics, 4th ed. Sage, London, UK.

Friedland K.D., Ama-Abasi D., Manning M., Clarke L., Kligys G., Chambers R.C. (2005). Automated egg counting and sizing from scanned images: Rapid sample processing and large data volumes for fecunidty estimates. Journal of Sea Research 54: 307-316.

Ganias K., Rakka M., Vavalidis T., Nunes C. (2010). Measuring batch fecundity using automated particle counting. Fisheries Research 106: 570-574

Gauthier D.T., Rhodes M.W. (2009). Mycobacteriosis in fishes: A review. The Veterinary Journal 180: 33-47

Gervasi C.L., Lowerre-Barbieri S.K., Vogelbein W.K., Gartland J., Latour R.J. (2019). The reproductive biology of Chesapeake Bay striped bass with consideration of the effects of mycobacteriosis. Bulletin of Marine Science 95(2): 117-137.

Giavarina D. (2015). Understanding Bland Altman analysis. Biochemia Medica 25(2): 141-151

Greeley Jr, M.S. (2002). Reproductive indicators of environmental stress in fish. Biological indicators of aquatic ecosystem stress, 321-377.

Hunter J.R., Macewicz B.J., Kimbrell C.A. (1989) Fecundity and other aspects of the reproduction of sablefish, *Anoplopoma fimbria*, in Central Californian waters. California Cooperative Fisheries Reports 30: 61-72

Iwanowicz D.D. (2011) Overview on the effects of parasites on fish health. *Third Bilateral Conference Between Russia and the United States, Aquatic Animal Health 2009*, Shepardstown, WV. Khaled bin Sultan Living Oceans Foundation, Landover, MD: p 176-184

Jackson L.F., Sullivan C.V. (1995). Reproduction of white perch: the annual gametogenic cycle. Transactions of the American Fisheries Society 124: 563-577

Jacobs J.M., Harrell R.M., Uphoff J., Townsend H., Hartman K. (2013). Biological reference points for the nutritional status of Chesapeake striped bass. North American Journal of Fisheries Management 33(3): 468-481.

Jacobs J.M., Stine C.B., Baya A.M., Kent M.L. (2009). A review of mycobacteriosis in marine fish. Journal of Fish Diseases 32: 119-130.

Kane A.S., Stine C.B., Hungerford L., Matsche M., Driscoll C., Baya A.M. (2007) Mycobacteria as environmental portent in Chesapeake Bay fish species. Emerging Infectious Diseases 13(2): 329-331

Kavanagh R.J., Balch G.C., Kiparissis Y., Niimi A.J., Sherry J., Tinson C., Metcalfe C.D. (2004) Endocrine disruption and altered gonadal development in white perch (*Morone americana*) from the lower Great Lakes Region. Environmental Health Perspectives 112(8): 898-902

Kerr L.A., Secor D.H., Piccoli P.M. (2009). Partial migration of fishes as exemplified by the estuarine-dependent white perch. Fisheries 34(3): 114-123.

King R.S., Beaman J.R., Whigham D.F., Baker M.E., Weller D.E. (2004) Watershed land use is strongly linked to PCBs in white perch in Chesapeake Bay subestuaries. Environmental Science and Technology 38: 6546-6552.

Klauda, R.J., McLaren J.B., Schmidt R.E., Dey W.P. (1988). Life history of white perch in the Hudson River estuary. American Fisheries Society Monograph 4: 69-88.

Klibansky N., Juanes F. (2008). Procedures for efficiently producing high-quality fecundity data on a small budget. Fisheries Research 89: 84-89.

Kraus R.T., Secor D.H. (2004) Dynamics of white perch Morone americana population contingents in the Patuxent River estuary, Maryland, USA. Marine ecology Progress series 279: 247-259.

Lambert Y. (2008). Why should we closely monitor fecundity in marine fish populations. Journal of Northwest Atlantic Fisheries Science 41: 93-106

LaPointe D., Vogelbein W.K., Fabrizio M.C., Gauthier D.T., Brill R.W. (2014) Temperature, hypoxia, and mycobacteriosis: effects on adult striped bass *Morone saxatilis* metabolic performance. Diseases of Aquatic Organisms 108: 113-127.

Lom J., Dyková I. (1981) Fish coccidia: critical notes on life cycles, classification and pathogenicity. Journal of Fish Diseases 4: 487-505.

Margulies D. (1990) Vulnerability of larval white perch, *Morone americana* to fish predation. Environmental Biology of Fishes 27: 187.

Mansueti R.J. (1961). Movements, reproduction, and mortality of the white perch, *Roccus americanus*, in the Patuxent estuary, Maryland. Chesapeake Science 2:142-205

Mansueti R.J. (1964). Eggs, larvae, and young of the white perch, *Roccus americanus*, with comments on its ecology in the estuary. Chesapeake Science 5: 3-45

Matsche M.A., Overton A., Jacobs J., Rhodes M.R., Rosemary K.M. (2010). Low prevalence of splenic mycobacteriosis in migratory striped bass *Morone*

saxatilis from North Carolina and Chesapeake Bay, USA. Diseases of Aquatic Organisms 90: 181-189.

Matsche M.A., Adams C.R., Blazer V.S. (2019a) Newly described coccidia *Goussia bayae* from white perch *Morone americana*: Morphology and phylogenetics support emerging taxonomy of *Goussia* within piscine hosts. Journal of Parasitology 105(1): 1-10

Matsche M.A., Blazer V.S., Mazik P.M. (2019b). Seasonal development of the coccidian parasite *Goussia bayae* and hepatobiliary histopathology in white perch *Morone americana* from Chesapeake Bay. Diseases of Aquatic Organisms 134:113-135

Matsche, M.A., Blazer V.S., Pulster E.L., Mazik P.M. (in press). "High prevalence of biliary neoplasia in white perch *Morone americana*: potential roles of bile duct parasites and environmental contaminants." Diseases of Aquatic Organisms.

McBride G.B. (2005). A proposal for strength-of-agreement criteria for Lin's concordance correlation coefficient. NIWA Client Report: HAM2005-062

McCollough C. (2019) Personal communication to the author. Email

McGrath P., Austin H.A. (2009) Site fidelity, home range, and tidal movements of white perch during the summer in two small tributaries of the York River, Virginia. Transactions of the American Fisheries Society 138: 966-974

McLaughlin S.M., Leight A.K., Spires J.E., Bricker S.B., Jacobs J.M., Messick G.A., Skelley S. (2018). Coastal Ecological Assessment to Support NOAA's Choptank River Complex Habitat Focus Area: Tred Avon River. NOAA Technical Memorandum NOS NCCOS 251. Oxford, MD 118 pp.

Monosson E., Fleming W.J., Sullivan C.V. (1994) Effects of the planar PCB 3,3',4,4'-tetrachlorobiphenyl (TCB) on ovarian development, plasma levels of sex steroid hormones and vitellogenin, and progeny survival in the white perch (*Morone americana*). Aquatic Toxicology 29: 1-19

Morgan R.P., Fleming R.F., Rasin V.J., Heinle D.R. (1973). Sublethal effects of Baltimore Harbor water on the white perch, *Morone americana*, and the hogchoker, *Trinectes maculatus*. Chesapeake Science 14(1): 17-27

Morrison C.M., Hawkins W.E. (1984) Coccidians in the liver and testis of the herring *Clupea harengus*. Canadian Journal of Zoology 62(3): 480-493

Murua H., Kraus G., Saborido-Rey F., Witthames P.R., Thorsen A., Junquera S. (2003) Procedures to estimate fecundity of marine fish species in relation to their reproductive strategy. Journal of Northwest Fishery Science 33: 33-54

Okoye A.O., Overton A.S., Loeffler M., Winslow S.E. (2008) White perch fecundity relationships in western Albemarle Sound, North Carolina. Journal of the North Carolina Academy of Science 124: 46-50

Overstreet R.M. (1997) Parasitological data as monitors of environmental health. Parassitologia 39: 169-175

Parveen, S., Jacobs, J., Ozbay, G., Chintapenta, L. K., Almuhaideb, E., Meredith, J., Ossai, S., Abbott, A., Brohawn, K., Chigbu, P., Richards, G. P. (2020). Seasonal and Geographical Differences in Total and Pathogenic Vibrio parahaemolyticus and Vibrio vulnificus Levels in Seawater and Oysters from the Delaware and Chesapeake Bays Determined Using Several Methods. Applied and Environmental Microbiology 86(23)

Piavis P., Webb III E. (2017). Population assessment of white perch in select regions of Chesapeake Bay, Maryland. *In* Chesapeake Bay finfish and habitat investigations. Maryland Department of Natural Resources. Report F-61-R. Annapolis, Maryland

Pinkney A.E., Harshbarger J.C., Karouna-Renier N.K., Jenko K., Balk L., Skarphéðinsdóttir H., Liewenborg B., Rutter M.A. (2011) Tumor prevalence and biomarkers of genotoxicity in brown bullhead (*Ameiurus nebulosus*) in Chesapeake Bay tributaries. Science of the Total Environment 410-411: 248-257

Pintor, J.M., Carrión P., Cernadas E., González-Rufino E., Formella A., Fernández-Delgado M., Domínguez-Petit R., Rábade-Uberos S. (2016). Govocitos: A software tool for estimating fish fecundity based on digital analysis of histological images. Computers and Electronics in Agriculture, 125: 89-98.

Poukish C. (2017) Personal communication to the author. Email

Richkus W.A., Stroup F. (1987) Characterization of the biology of and fisheries for Maryland stocks of white perch. Maryland Dept. of Natural Resources, Tidal Fisheries Div. Annapolis, MD.

Roberts, R. J. (2012). Fish pathology. John Wiley & Sons.

Saborido-Rey F., Trippel E.A. (2013). Fish reproduction and fisheries. Fisheries Research 138: 1-4.

Scherle, W. (1970). A simple method for volumetry of organs in quantitative stereology. Mikroskopie 26: 57-60.

Schreck C.B., Contreras-Sanchez W., Fitzpatrick M.S. (2001). Effects of stress on fish reproduction, gamete quality, and progeny. In Reproductive Biotechnology in Finfish Aquaculture (pp. 3-24). Elsevier.

Schreck C.B., Moyle P.B., eds. (1990) Methods for Fish Biology

Scott W.B., Christie W.J. (1963). The invasion of the lower Great Lakes by the white perch, *Roccus americanus*, Journal of the Fisheries Research Board of Canada. 20: 1189-1195.

Setzler-Hamilton E., (1991) White Perch, *Morone americana,* In: Funderbunk S.L., Mihursky J.A., Jordan S.J., Riley D. (eds) Habitat requirements for Chesapeake Bay living resources, 2nd edn. Chesapeake Research Consortium, Solomons, p 12-1-12-20

Stanley J.G., Danie D.S. (1983). Species Profile: life histories and environmental requirements of coastal fishes and invertebrates (North Atlantic): white perch. US Fish and Wildlife Service, Div. Biol. Serv., FWS/OBS-82/11.7: 1-12

Tanaka H., Hamatsu T., Mori K. (2017). Comparison of potential fecundity models for walleye pollock *Gadus chalcogrammus* in the Pacific waters off Hokkaido, Japan. Journal of Fish Biology 90: 236-248

Taub, S.H. (1969). Fecundity of the white perch. The Progressive Fish Culturist 31(3): 166-168.

Thorsen A., Kjesbu O.S. (2001). A rapid method for estimation of oocyte size and potential fecundity in Atlantic cod using a computer-aided particle analysis system. Journal of Sea Research 46: 295-308.

Uphoff J.H., McGinty M., Lukacovic R., Mowrer J., Pyle B. (2011) Impervious surface, summer dissolved oxygen, and fish distribution in Chesapeake Bay

subestuaries: Linking watershed development, habitat conditions and fisheries management, North American Journal of Fisheries Management 31: 554-566

USEPA. Guidance for federal land management in the Chesapeake Bay watershed. Chapter 2: Agriculture. Rep. EPA841-R-10–002. In USEPA, Nonpoint Source Pollution, Office of Wetlands, Oceans, and Watersheds, 2010.

USFWS and AFS-FHS (U.S. Fish and Wildlife Service and American Fisheries Society-Fish Health Section). 2014. Standard procedures for aquatic animal health inspections. In AFS-FHS. FHS blue book: suggested procedures for the detection and identification of certain finfish and shellfish pathogens, 2016 edition. Accessible at: http://afsfhs.org/bluebook/bluebook-index.php.

Walter J.F., Austin H.M. (2003). Diet composition of large striped bass (*Morone saxatilis*) in Chesapeake Bay, Fisheries Bulletin 101: 414-423

Webb, E. (2018) Personal communication to the author. Email

West M.J. (2012). Basic Stereology for Biologists and Neuroscientists. Cold Spring Harbor Laboratory Press, Cold Spring Harbor, New York.

Weibel E.R., Gomez D.M. (1962) Special communications. A principle for counting tissue structures on random sections. Journal of Applied Physiology 17: 343-348

Witthames P.R. (2003). Methods to assess maturity and realized fecundity illustrated by studies on Dover sole *Solea solea*. Modern approaches to assess maturity and fecundity of warm and cold-water fish and squids.

Yonkos, L. T., Friedel, E. A., Fisher, D. J. (2014). Intersex (testicular oocytes) in largemouth bass (Micropterus salmoides) on the Delmarva Peninsula, USA. Environmental toxicology and chemistry, 33(5): 1163-1169.

Zuerlein, G. (1981). The White Perch, Marone americana (Gmelin) in Nebraska.